of cardiac and renal sympathetic nerve activities. *Am J Physiol Heart Circ Physiol* 280: H1581–H1590, 2001.

16. **Kawada T, Yamamoto K, Kamiya A, Ariumi H, Michikami D, Shishido T, Sunagawa K, Sugimachi M.** Dynamic characteristics of carotid sinus pressure-nerve activity transduction in rabbits. *Jpn J Physiol* 55: 157–163, 2005.
17. **Kawada T, Yanagiya Y, Uemura K, Miyamoto T, Zheng C, Li M, Sugimachi M, Sunagawa K.** Input-size dependence of the baroreflex neural arc transfer characteristics. *Am J Physiol Heart Circ Physiol* 284: H404–H415, 2003.
18. **Kawada T, Sugimachi M, Sato T, Miyano H, Shishido T, Miyashita H, Yoshimura R, Takaki H, Alexander J Jr, Sunagawa K.** Closed-loop identification of carotid sinus baroreflex open-loop transfer characteristics. *Am J Physiol Heart Circ Physiol* 273: H1024–H1031, 1997.
19. **Lohmeier TE, Iliescu R, Dwyer TM, Irwin ED, Cates AW, Rossing MA.** Sustained suppression of sympathetic activity and arterial pressure during chronic activation of the carotid baroreflex. *Am J Physiol Heart Circ Physiol* 299: H402–H409, 2010.
20. **Marmarelis PZ, Marmarelis VZ.** The white noise method in system identification. In: *Analysis* of Physiological Systems. New York: Plenum, 131–180, 1978.
21. **Mills E, Bruckert JW.** Pressor mechanisms linked obligatorily to spontaneous hypertension in the rat. *Hypertension* 11: 427–432, 1988.
22. **Mizuno M, Kawada T, Kamiya A, Miyamoto T, Shimizu S, Shishido T, Smith SA, Sugimachi M.** Dynamic characteristics of heart rate control by the autonomic nervous system in rats. *Exp Physiol* 95: 919–925, 2010.
23. **Mohrman DE, Heller LJ.** *Cardiovascular Physiology* **(6th ed).** New York: McGraw Hill, 2006, p. 172–177, 2006.
24. **Nosaka S, Wang SC.** Carotid sinus baroreceptor functions in the spontaneously hypertensive rat. *Am J Physiol* 222: 1079–1084, 1972.
25. **Liu HK, Guild SJ, Ringwood JV, Barrett CJ, Leonard BL, Nguang SK, Navakatikyan MA, Malpas SC.** Dynamic baroreflex control of blood pressure: influence of the heart vs. peripheral resistance. *Am J Physiol Regul Integr Comp Physiol* 283: R533–R542, 2002.
26. **Osborn JW.** Pathogenesis of hypertension in the sinoaortic-denervated spontaneously hypertensive rat. *Hypertension* 18: 475–482, 1991.
27. **Rho JH, Newman B, Alexander N.** Altered in vitro uptake of norepinephrine by cardiovascular tissues of spontaneously hypertensive rats. Part 1. In: *Mesenteric Artery Hypertension* 3: 704–709, 1981.
28. **Rho JH, Newman B, Alexander N.** Altered in vitro uptake of norepinephrine by cardiovascular tissues of spontaneously hypertensive rats. Part 2. Portal-mesenteric veins and atria. *Hypertension* 3: 710–717, 1981.
29. **Salgado HC, Barale AR, Castania JA, Machado BH, Chapleau MW, Fazan R Jr.** Baroreflex responses to electrical stimulation of aortic depressor nerve in conscious SHR. *Am J Physiol Heart Circ Physiol* 292: H593–H600, 2007.
30. **Sapru HN, Wang SC.** Modification of aortic baroreceptor resetting in the spontaneously hypertensive rat. *Am J Physiol* 230: 664–674, 1976.
31. **Sato T, Kawada T, Inagaki M, Shishido T, Sugimachi M, Sunagawa K.** Dynamics of sympathetic baroreflex control of arterial pressure in rats. *Am J Physiol Regul Integr Comp Physiol* 285: R262–R270, 2003.
32. **Sato T, Kawada T, Miyano H, Shishido T, Inagaki M, Yoshimura R, Tatewaki T, Sugimachi M, Alexander J Jr, Sunagawa K.** New simple methods for isolating baroreceptor regions of carotid sinus and aortic depressor nerves in rats. *Am J Physiol Heart Circ Physiol* 276: H326–H332, 1999.
33. **Sato T, Kawada T, Sugimachi M, Sunagawa K.** Bionic technology revitalizes native baroreflex function in rats with baroreflex failure. *Circulation* 106: 730–734, 2002.
34. **Shoukas AA, Callahan CA, Lash JM, Haase EB.** New technique to completely isolate carotid sinus baroreceptor regions in rats. *Am J Physiol Heart Circ Physiol* 260: H300–H303, 1991.
35. **Ursino M, Fiorenzi A, Belardinelli E.** The role of pressure pulsatility in the carotid baroreflex control: a computer simulation study. *Comput Biol Med* 26: 297–314, 1996.
36. **Yamaguchi I, Kopin IJ.** Blood pressure, plasma catecholamines, and sympathetic outflow in pithed SHR and WKY rats. *Am J Physiol Heart Circ Physiol* 238: H365–H372, 1980.

33rd Annual International Conference of the IEEE EMBS
Boston, Massachusetts USA, August 30 - September 3, 2011

Consideration on Step Duration to Assess Open-loop Static Characteristics of the Carotid Sinus Baroreflex in Rats

Toru Kawada, Shuji Shimizu, Yusuke Sata, Atsunori Kamiya, Kenji Sunagawa, and Masaru Sugimachi

Abstract—**The carotid sinus baroreflex is one of the most important negative feedback systems to stabilize arterial pressure. Although static characteristics of the carotid sinus baroreflex can be assessed by using a stepwise input protocol under baroreflex open-loop conditions, the step duration has been determined empirically. In the present study, we examined the effects of different time windows (5-10, 15-20, 25-30, 35-40, 45-50, and 55-60 s) on the static characteristics estimated by using a 60-s stepwise input protocol in 10 anesthetized rats. Based on the results, we compared the static characteristics between actual 60-s and 20-s stepwise input protocols. Most of the parameters of the static characteristics did not differ significantly between the 60-s and 20-s stepwise input protocols, suggesting that the open-loop baroreflex static characteristics can be estimated by using a stepwise input with the step duration as short as 20 s in normal rats.**

I. Introduction

The carotid sinus baroreflex system is one of the most important negative feedback systems to stabilize arterial pressure (AP). The carotid sinus baroreflex may be divided into two principal subsystems [1], [2]. One is a neural arc subsystem that acts as a controller for regulating sympathetic nerve activity (SNA) in response to a baroreceptor pressure input. The other is a peripheral arc subsystem that serves as a plant for yielding AP according to SNA through cardiovascular responses. In order to assess the open-loop static characteristics of these two subsystems, a stepwise (staircase-wise) input has been employed. The levels of input pressure are changed stepwise to cover the whole input pressure range of the arterial baroreflex, e.g., between 60 and 180 mmHg in rats. Each input pressure level is sustained for certain duration to make the system response reach steady state at a given input pressure level. Empirically, 60-s step duration seems to be appropriate for estimating the baroreflex static characteristics in rats [3], [4]. Although minimizing the step duration would contribute to shortening the total experimental time, too short duration can violate the assumption of acquiring the steady-state response. In the present study, we examined possible shortest step duration necessary for estimating the baroreflex open-loop static characteristics in rats.

Manuscript received March 20, 2011. This work was supported in part by Health and Labour Sciences Research Grants (H19-nano-Ippan-009, H20-katsudo-Shitei-007, H21-nano-Ippan-005) from the Ministry of Health, Labour and Welfare of Japan.

T. Kawada, S. Shimizu, Y. Sata, and M. Sugimachi are with the Department of Cardiovascular Dynamics, National Cerebral and Cardiovascular Center, 565-8565 Osaka, Japan (corresponding author: T. Kawada, phone: +81-6-6833-5012, fax: +81-6-6835-5403, e-mail: torukawa@res.ncvc.go.jp).

K. Sunagawa is with the Department of Cardiovascular Medicine, Graduate School of Medical Sciences, Kyushu University, Fukuoka 812-8582, Japan.

II. Materials and Methods

A. Animal Preparation

Animals were cared for in strict accordance with the *Guiding Principles for the Care and Use of Animals in the Field of Physiological Sciences*, which has been approved by the Physiological Society of Japan. All experimental protocols were reviewed and approved by the Animal Subjects Committee at National Cerebral and Cardiovascular Center.

The study was conducted using ten male Sprague-Dawley rats. Each rat was anesthetized by an intraperitoneal injection (2 ml/kg) of a mixture of urethane (250 mg/ml) and α-chloralose (40 mg/ml), and mechanically ventilated through a tracheal tube with oxygen-enriched room air. A venous catheter was inserted into the right femoral vein for a maintenance dose of the above anesthetic mixture diluted by 20 fold (2-3 $ml \cdot kg^{-1} \cdot h^{-1}$). An arterial catheter was inserted into the right femoral artery to measure AP, from which heart rate (HR) was detected. Another venous catheter was inserted into the left femoral vein for the infusion of Ringer solution (6 $ml \cdot kg^{-1} \cdot min^{-1}$) to maintain fluid balance.

In order to record SNA, a postganglionic branch from the splanchnic sympathetic nerve was exposed through a left flank incision. A pair of stainless steel wire electrodes (Bioflex wire, AS633, Cooner Wire, CA, USA) was attached to the nerve, and the nerve and electrodes were covered with silicone glue (Kwik-Sil, World Precision Instruments, FL, USA). To quantify the nerve activity, the preamplified signal was band-pass filtered at 150-1000 Hz, and was full-wave rectified and low-pass filtered with a cut-off frequency of 30 Hz. Pancuronium bromide (0.4 $mg \cdot kg^{-1} \cdot h^{-1}$) was administered to prevent muscular activity from contaminating the SNA recording. At the end of the experiment, an intravenous bolus injection of a ganglionic blocker, hexamethonium bromide (60 mg/kg), was given to confirm the disappearance of SNA. The noise level was then recorded and served as zero SNA. Because the absolute magnitude of SNA varied among animals depending on recording conditions, mean SNA value corresponding to the carotid sinus pressure (CSP) of 60 mmHg calculated at the time window of 55-60 s was assigned to be 100 au (arbitrary units).

Bilateral vagal and aortic depressor nerves were sectioned at the neck to avoid reflexes from the cardiopulmonary region

and aortic arch. The carotid sinus regions were isolated from the systemic circulation using previously reported procedures [5], [6] with modifications. A 7-0 polypropylene suture with a fine needle (PROLENE, Ethicon, GA, USA) was passed through the tissue between the external and internal carotid arteries, and the external carotid artery was ligated close to the carotid bifurcation. The internal carotid artery was embolized by the injection of two to three steel balls with a diameter of 0.8 mm (Tsubaki Nakashima, Nara, Japan) via the common carotid artery. The isolated carotid sinuses were filled with warmed Ringer solution via the catheter inserted into the common carotid arteries. CSP was controlled using a servo-controlled piston pump. Heparin sodium (100 U/kg) was given intravenously to prevent blood coagulation. Body temperature was maintained at approximately 38°C with a heating pad and a lamp.

B. Estimation of Baroreflex Open-loop Static Characteristics Using Different Time Windows in a 60-s Stepwise Input

To estimate the open-loop static characteristics of the total baroreflex, neural arc, peripheral arc, and HR control, CSP was first decreased to 60 mmHg for four min, and increased stepwise from 60 to 180 mmHg at increments of 20 mmHg every minute.

Mean values of SNA, AP, and HR were calculated from time windows of 5-10, 15-20, 25-30, 35-40, 45-50, and 55-60 s at each CSP level. In each rat, data from two consecutive 60-s stepwise input cycles were averaged. The static characteristics of the total baroreflex (the CSP-AP relationship), neural arc (the CSP-SNA relationship), and HR control (the CSP-HR relationship) were quantified using a four-parameter logistic function as [7]:

$$y = \frac{P_1}{1+\exp[P_2(x-P_3)]} + P_4$$

where x and y denote the input and output values, respectively; P_1 is the response range; P_2 is the slope coefficient, P_3 is the midpoint input pressure; and P_4 is the minimum value of the output.

The static characteristics of the baroreflex peripheral arc (the SNA-AP relationship) were quantified by a linear regression analysis as:

$$AP = a \times SNA + b$$

where a and b represent the slope and intercept, respectively.

C. Estimation of Baroreflex Open-loop Static Characteristics Using a 20-s Stepwise Input

Based on preliminary results of the open-loop static characteristics using different time windows in a 60-s stepwise input described above, the system response to a 20-s stepwise input was examined. The 20-s stepwise input protocol was conducted before (n = 5) or after (n = 5) the 60-s stepwise input protocol to make the possible time effect be even between the two protocols. Mean values of SNA, AP, and HR were obtained during the last 5 s (15-20 s) at each CSP level. In each rat, data from two consecutive 20-s stepwise input cycles were averaged.

D. Statistical Analysis

All data are expressed as means±SE values. To compare the effects of differing the time windows of analysis (5-10, 15-20, 25-30, 35-40, 45-50, and 55-60 s) on the parameters of the baroreflex static characteristics, repeated-measures analysis of variance (ANOVA) was used [8]. If there was a significant difference, a Dunnett's test was applied to identify the difference against the data calculated from a time window of 55-60 s. To compare the parameters of the baroreflex static characteristics between the 60-s and 20-s stepwise input protocols, a paired-t test was used. Differences were considered to be significant when $P < 0.05$. We used a rule of thumb that the parameters derived from two protocols were considered to be similar when $P > 0.2$.

III. Results and Discussion

Fig. 1 represents typical recordings of CSP, SNA, AP, and HR during 60-s and 20-s stepwise input protocols. A white line in the SNA recording is a 2-s moving averaged signal. An increase in CSP decreased SNA, AP, and HR. The maximum and minimum values of SNA, AP, and HR responses did not differ significantly between the two input protocols.

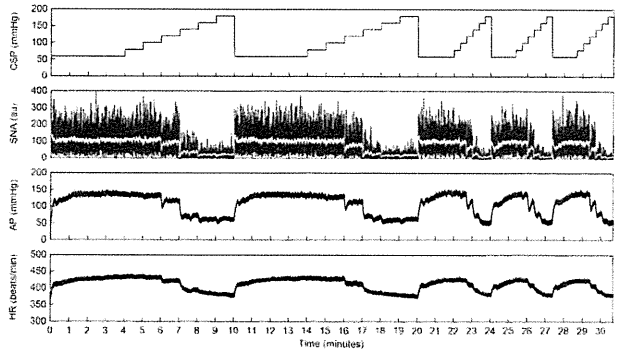

Fig. 1. Typical experimental recordings during 60-s and 20-s stepwise input protocols. CSP: carotid sinus pressure, SNA: sympathetic nerve activity, AP: arterial pressure, HR: heart rate. The white line in the SNA recording represents a 2-s moving averaged signal.

Figure 2 (the last page) summarizes the open-loop static characteristics of the total baroreflex, neural arc, peripheral arc, and HR control, obtained from the 60-s stepwise input protocol, with the analyses using different time windows. The characteristics of the total baroreflex, neural arc, and HR control approximated an inverse sigmoid curve. The characteristics of the peripheral arc approximated a straight line. The data obtained during 55-60 s served as controls. The estimated parameter values, except those estimated during 5-10 s, did not differ significantly from those obtained during 55-60 s (Table 1), suggesting that the open-loop static characteristics of the baroreflex could be obtained using a stepwise input with step duration as short as 20 s.

Figure 3 (the last page) compares the open-loop static characteristics of the total baroreflex, neural arc, peripheral arc, and HR control between actually applied 20-s and 60-s stepwise input protocols. Data were calculated from the last 5 s of each step. The lines of mean data obtained from the two protocols were very close (Fig. 3, right panels, dashed line: 20-s, solid line: 60-s). In the parameters of the total baroreflex, no significant differences were detected between the two protocols (Table 2). In the neural arc, although the slope coefficient was significantly smaller by 0.006 in the 20-s stepwise input protocol, the magnitude of the difference was comparable to the corresponding SE value (0.006) in the 60-s stepwise input protocol. Other parameters of the neural arc did not differ significantly. Parameters of the peripheral arc did not differ significantly between the two protocols. In the HR control, although the response range was significantly smaller by 3.6 beats/min in the 20-s stepwise input protocol, the magnitude of the difference was less than the corresponding SE value (7.5 beats/min) in the 60-s stepwise input protocol. Other parameters did not differ significantly. Although we did not carry out an equivalence test, if we use a rule of thumb that the two parameter values are considered to be similar when $P > 0.2$, the midpoint input pressure (P_3) could be different in all of the total baroreflex, neural arc, and the HR control. The percent difference of P_3 values relative to the value estimated by the 60-s stepwise input protocol was, however, less than 5% on the average. Collectively, although several parameters differed slightly, the 20-s stepwise input protocol provided parameter values similar to those obtained from the 60-s stepwise input protocol. The differences of the parameters between the two protocols could not be detected if we applied an unpaired-t test instead of a paired-t test, suggesting that the detected difference was within the inter-individual variations.

Although too short step duration in a stepwise input protocol will violate the assumption that the system's steady-state response is obtained, too long step duration will also violate the assumption that the system remains stationary. Minimizing the step duration may contribute to shortening the total experimental time and making the assumption for stationarity more feasible in biological experiment. In addition, when examining the effects of certain interventions on the system characteristics, reducing the step duration would increase the time resolution for tracking the effects of interventions on the system characteristics. In other words, by using a 20-s stepwise input protocol, we may be able to increase the time resolution of the systems analysis by 3 fold compared to a 60-s stepwise input protocol.

There is a limitation to the present study. We estimated the baroreflex static characteristics in normal anesthetized rats. In diseased conditions such as chronic heart failure, the cardiovascular responses could be blunted [3]. In such conditions, longer step duration may be required for AP to reach a new steady state at a given input pressure, and thus the 20-s stepwise input protocol may not work well. Apparently, some priori knowledge or preliminary studies are needed to use the 20-s rather than the 60-s stepwise input protocol.

IV. Conclusion

The open-loop static characteristics of the carotid sinus baroreflex in normal rats may be obtained by the stepwise input protocol with step duration as short as 20 s. The shortening of the step duration can reduce the total amount of experimental time. Moreover, it would also make it possible to analyze the time effect of drugs on the baroreflex static characteristics with a better time resolution.

References

[1] D. E. Mohrman, L. J. Heller. Cardiovascular Physiology, 6th ed. New York: Lange Medical Books/McGraw-Hill, 2006, pp. 172–177.

[2] T. Sato, T. Kawada, M. Inagaki, T. Shishido, H. Takaki, M. Sugimachi, et al. "New analytic framework for understanding sympathetic baroreflex control of arterial pressure," *Am. J. Physiol.*, vol. 276, pp. H2251-H2261, 1999.

[3] T. Kawada, M. Li, A. Kamiya, S. Shimizu, K. Uemura, H. Yamamoto, et al. "Open-loop dynamic and static characteristics of the carotid sinus baroreflex in rats with chronic heart failure after myocardial infarction," *J. Physiol. Sci.*, vol. 60, pp. 283-298, 2010.

[4] T. Kawada, A. Kamiya, M. Li, S. Shimizu, K. Uemura, H. Yamamoto, et al. "High levels of circulating angiotensin II shift the open-loop baroreflex control of splanchnic sympathetic nerve activity, heart rate and arterial pressure in anesthetized rats," *J. Physiol. Sci.*, vol. 59, pp. 447-455, 2010.

[5] A. A. Shoukas, C. A. Callahan, J. M. Lash, E. B. Haase. "New technique to completely isolate carotid sinus baroreceptor regions in rats," *Am. J. Physiol. Heart Circ. Physiol.*, vol. 260, pp. H300-H303, 1991.

[6] T. Sato, T. Kawada, H. Miyano, T. Shishido, M. Inagaki, R. Yoshimura, et al. "New simple methods for isolating baroreceptor regions of carotid sinus and aortic depressor nerves in rats," *Am. J. Physiol. Heart Circ. Physiol.*, vol. 276, pp. H326-H332, 1999.

[7] B. B. Kent, J. W. Drane, B. Blumenstein, J. W. Manning. "A mathematical model to assess changes in the baroreceptor reflex," *Cardiology.*, vol. 57, pp. 295-310, 1972.

[8] S. A. Glantz, Primer of Biostatistics, 5th ed. New York: McGraw-Hill, 2002, pp. 318-329.

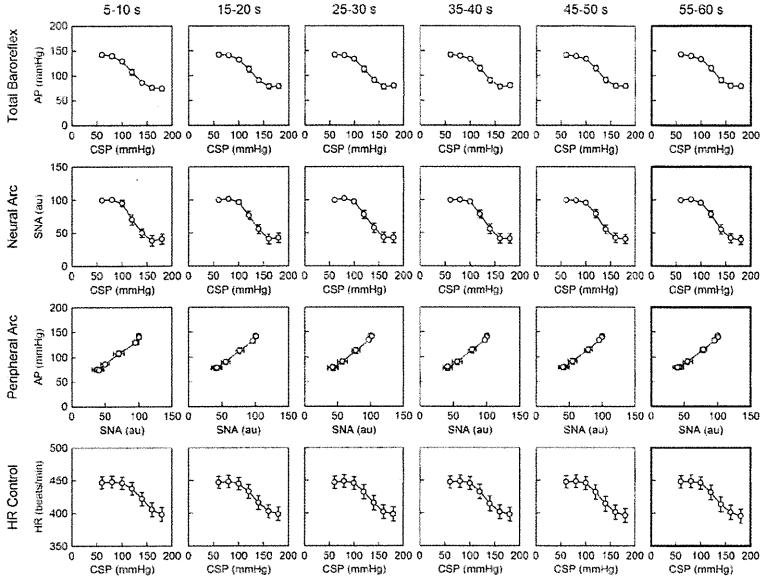

Fig. 2. Open-loop static characteristics of the carotid sinus baroreflex estimated at different time windows of the 60-s stepwise input protocol. CSP: carotid sinus pressure, AP: arterial pressure, SNA: sympathetic nerve activity, HR: heart rate. The rightmost panels serve as controls.

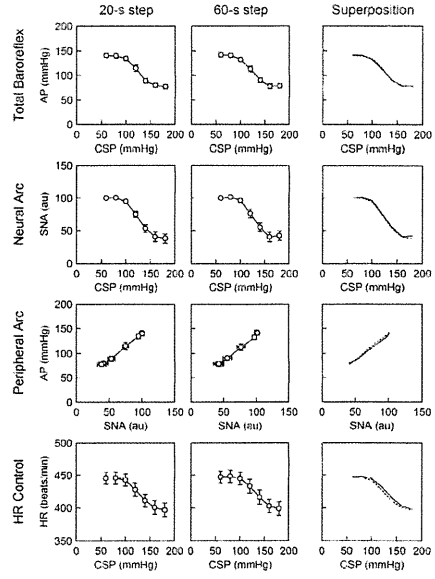

Fig. 3. Open-loop static characteristics of the carotid sinus baroreflex estimated using 20-s and 60-s stepwise input protocols. CSP: carotid sinus pressure, AP: arterial pressure, SNA: sympathetic nerve activity, HR: heart rate.

Table 1. Parameters of open-loop static characteristics of the carotid sinus baroreflex estimated at different time windows in the 60-s stepwise input protocol.

	5-10 s	15-20 s	25-30 s	35-40 s	45-50 s	55-60 s
Total Baroreflex						
P_1, mmHg	72.5±8.6**	68.8±8.0	67.9±7.8	66.4±7.7	65.0±7.8	65.4±7.1
P_2, mmHg^{-1}	0.088±0.011	0.089±0.009	0.095±0.011	0.099±0.009	0.097±0.009	0.091±0.008
P_3, mmHg	118.1±3.6**	122.1±3.5	122.8±3.6	123.6±3.5	124.0±3.6	123.7±3.6
P_4, mmHg	72.9±4.8**	74.9±5.2	75.1±5.2	75.5±5.1	76.2±5.1	76.3±4.8
Neural Arc						
P_1, au	65.5±7.6	63.0±6.7	62.6±8.0	62.8±7.3	61.3±7.1	63.1±6.5
P_2, mmHg^{-1}	0.115±0.014	0.102±0.012	0.102±0.010	0.100±0.009	0.101±0.010	0.088±0.006
P_3, mmHg	120.6±3.6**	125.1±3.7	126.0±3.8	127.8±3.8	127.2±3.6	127.0±3.6
P_4, au	37.6±7.8	39.3±7.4	40.1±8.1	38.4±7.3	39.3±7.1	38.7±6.7
Peripheral Arc						
a, mmHg/au	1.06±0.07	1.06±0.07	1.10±0.07	1.09±0.08	1.07±0.07	1.06±0.07
b, mmHg	31.0±7.4	31.2±6.9	27.0±8.0	29.4±8.1	32.0±6.4	32.1±7.0
HR Control						
P_1, beats/min	52.8±8.2	51.8±8.4	52.3±8.2	51.7±8.0	53.8±8.0	54.8±7.5
P_2, mmHg^{-1}	0.077±0.006	0.082±0.008	0.089±0.010	0.093±0.009	0.087±0.008	0.083±0.007
P_3, mmHg	138.5±2.9**	131.0±3.1	131.0±3.4	130.5±3.3	131.1±3.6	130.8±3.5
P_4, beats/min	395.7±10.8	397.2±10.4	396.8±10.8	397.4±10.3	395.7±10.6	395.2±10.5

Data are means±SE values. **P < 0.01 by Dunnett's test from the value estimated at a time window of 55-60 s.

Table 2. Parameters of open-loop static characteristics of the carotid sinus baroreflex estimated by actual 20-s and 60-s stepwise input protocols.

	20-s step	60-s step	P value	%difference
Total Baroreflex				
P_1, mmHg	65.9±7.5	65.4±7.1	0.779	0.1±3.5
P_2, mmHg^{-1}	0.094±0.009	0.091±0.008	0.691	1.0±8.1
P_3, mmHg	121.9±3.0	123.7±3.6	0.148	1.4±0.9
P_4, mmHg	76.6±4.3	76.3±4.8	0.893	−0.4±2.0
Neural Arc				
P_1, au	65.5±7.6	63.1±6.5	0.330	−1.5±4.5
P_2, mmHg^{-1}	0.082±0.008*	0.088±0.006	0.011	10.8±3.8
P_3, mmHg	121.8±3.3	127.0±3.6	0.075	4.4±2.3
P_4, au	37.4±7.2	38.7±6.7	0.414	9.6±7.5
Peripheral Arc				
a, mmHg/au	1.09±0.08	1.06±0.07	0.351	−1.1±2.5
b, mmHg	31.4±8.3	32.1±7.0	0.780	7.3±11.1
HR Control				
P_1, beats/min	51.2±8.2*	54.8±7.5	0.041	13.7±7.6
P_2, mmHg^{-1}	0.082±0.008	0.083±0.007	0.820	6.6±8.9
P_3, mmHg	126.5±3.3	130.8±3.5	0.126	3.5±2.1
P_4, beats/min	396.4±10.4	395.2±10.5	0.501	−0.3±0.4

Data are means±SE values. *P < 0.05 by a paired-t test.

Circulation Journal
Official Journal of the Japanese Circulation Society
http://www.j-circ.or.jp

ORIGINAL ARTICLE
Hypertension and Circulatory Control

Medetomidine, an α_2-Adrenergic Agonist, Activates Cardiac Vagal Nerve Through Modulation of Baroreflex Control

Shuji Shimizu, MD, PhD; Tsuyoshi Akiyama, MD, PhD; Toru Kawada, MD, PhD; Yusuke Sata, MD; Masaki Mizuno, PhD; Atsunori Kamiya, MD, PhD; Toshiaki Shishido, MD, PhD; Masashi Inagaki, MD; Mikiyasu Shirai, MD, PhD; Shunji Sano, MD, PhD; Masaru Sugimachi, MD, PhD

Background: Although α_2-adrenergic agonists have been reported to induce a vagal-dominant condition through suppression of sympathetic nerve activity, there is little direct evidence that they directly increase cardiac vagal nerve activity. Using a cardiac microdialysis technique, we investigated the effects of medetomidine, an α_2-adrenergic agonist, on norepinephrine (NE) and acetylcholine (ACh) release from cardiac nerve endings.

Methods and Results: A microdialysis probe was implanted into the right atrial wall near the sinoatrial node in anesthetized rabbits and perfused with Ringer's solution containing eserine. Dialysate NE and ACh concentrations were measured using high-performance liquid chromatography. Both 10 and 100 μg/kg of intravenous medetomidine significantly decreased mean blood pressure (BP) and the dialysate NE concentration, but only 100 μg/kg of medetomidine enhanced ACh release. Combined administration of medetomidine and phenylephrine maintained mean BP at baseline level, and augmented the medetomidine-induced ACh release. When we varied the mean BP using intravenous administration of phenylephrine, treatment with medetomidine significantly steepened the slope of the regression line between mean BP and log ACh concentration.

Conclusions: Medetomidine increased ACh release from cardiac vagal nerve endings and augmented baroreflex control of vagal nerve activity. (*Circ J* 2012; **76:** 152–159)

Key Words: Acetylcholine; Norepinephrine; Sinoatrial node; Sympathetic nervous system; Vagus nerve

The selective α_2-adrenergic agonist, dexmedetomidine, is widely used for sedation in intensive care units because it has a less respiratory depressive effect.[1] In addition, several benefits of dexmedetomidine that favor its use in intensive care have been reported, such as reduced opioid dosage requirement. In animal studies, Hayashi et al reported that dexmedetomidine prevented epinephrine-induced arrhythmias in halothane-anesthetized dogs.[2] This antiarrhythmic effect of α_2-adrenergic agonists may be partly ascribed to vagal activation.[3] It has already been reported that central sympathetic inhibition by an α_2-adrenergic agonist, guanfacine, augmented the sleep-related ultradian rhythm of parasympathetic tone in patients with chronic heart failure.[4] Although α_2-adrenergic agonists are widely recognized as inducing a vagal-dominant condition through the suppression of sympathetic nerve, there is little direct evidence that they directly increase cardiac vagal nerve activity, because such activity has been assessed only by indirect methods, such as heart rate variability, in most studies.[5]

Vanoli et al[6] reported that vagal stimulation after an acute ischemic episode effectively prevented ventricular fibrillation in dogs. Their group also indicated that the dogs that developed ventricular fibrillation during the acute ischemic episode had a significantly lower baroreflex-mediated heart rate response,[7] suggesting the importance of the baroreflex in controlling vagal function. If an α_2-adrenergic agonist is able to activate the cardiac vagal nerve directly or via modulation of the baroreflex function, it will provide a new therapeutic option for life-threatening arrhythmias after myocardial ischemia.

Medetomidine is a racemic mixture of 2 stereoisomers, dexmedetomidine and levomedetomidine. However, because it has already been reported that levomedetomidine has no effect on cardiovascular parameters and causes no apparent sedation or analgesia,[8] the pharmacokinetics of dexmedetomidine and racemic medetomidine are almost similar. We hypothesized that medetomidine can activate the cardiac vagal nerve

Received June 1, 2011; revised manuscript received September 6, 2011; accepted September 14, 2011; released online October 29, 2011
Time for primary review: 25 days

Department of Cardiovascular Dynamics (S. Shimizu, T.K., Y.S., M.M., A.K., T.S., M.I., M. Sugimachi), Department of Cardiac Physiology (T.A., M. Shirai), National Cerebral and Cardiovascular Center Research Institute, Suita; and Department of Cardiovascular Surgery, Okayama University Graduate School of Medicine, Dentistry and Pharmaceutical Sciences, Okayama (S. Sano), Japan
Mailing address: Shuji Shimizu, MD, PhD, Department of Cardiovascular Dynamics, National Cerebral and Cardiovascular Center Research Institute, 5-7-1 Fujishiro-dai, Suita 565-8565, Japan. E-mail: shujismz@ri.ncvc.go.jp

ISSN-1346-9843 doi:10.1253/circj.CJ-11-0574

through a central action and improve the baroreflex control of vagal nerve activity. We have established a cardiac microdialysis technique for separate monitoring of neuronal norepinephrine (NE) and acetylcholine (ACh) release to the rabbit sinoatrial (SA) node in vivo.[9–11] Using this microdialysis technique, we investigated the effects of medetomidine on cardiac autonomic nerve activities innervating the SA node.

Methods

Surgical Preparation

Animal care was provided in accordance with the "Guiding principles for the care and use of animals in the field of physiological sciences" published by the Physiological Society of Japan. All protocols were approved by the Animal Subject Committee of the National Cerebral and Cardiovascular Center.

In this study, 31 Japanese white rabbits weighing 2.3–3.0 kg were used. Anesthesia was initiated by an intravenous injection of pentobarbital sodium (50 mg/kg) via the marginal ear vein, and then maintained at an appropriate level by continuous intravenous infusion of α-chloralose and urethane (16 mg·kg^{-1}·h^{-1} and 100 mg·kg^{-1}·h^{-1}) through a catheter inserted into the femoral vein. The animals were intubated and ventilated mechanically with room air mixed with oxygen. Respiratory rate and tidal volume were set at 30 cycles/min and 15 ml/kg, respectively. Systemic arterial pressure was monitored by a catheter inserted into the femoral artery. Esophageal temperature, which was measured by a thermometer (CTM-303, Terumo, Japan), was maintained between 38°C and 39°C using a heating pad.

With the animal in lateral position, a right lateral thoracotomy was performed and the right 3rd to 5th ribs were partially resected to expose the heart. After incising the pericardium, a dialysis probe was implanted as described below. Three stainless steel electrodes were attached around the thoracotomy incision for recording body surface electrocardiogram (ECG). The heart rate was determined from the ECG using a cardiotachometer. Heparin sodium (100 IU/kg) was administered intravenously to prevent blood coagulation. At the end of the experiment, the animal was killed humanely by injecting an overdose of pentobarbital sodium. In the postmortem examination, the right atrial wall was resected en bloc with the dialysis probe. The inside of the atrial wall was observed macroscopically to confirm that the dialysis membrane was not exposed to the right atrial lumen.

Dialysis Technique

The materials and properties of the dialysis probe have been described previously.[9–12] A dialysis fiber of semipermeable membrane (length 4 mm, outer diameter 310 μm, inner diameter 200 μm, PAN-1200, molecular weight cutoff 50,000; Asahi Chemical, Tokyo, Japan) was attached at both ends to polyethylene tubes (length 25 cm, outer diameter 500 μm, inner diameter 200 μm). A fine guiding needle (length 30 mm, outer diameter 510 μm, inner diameter 250 μm) with a stainless steel rod (length 5 mm, outer diameter 250 μm) was used for the implantation of the dialysis probe. A dialysis probe was implanted into the right atrial myocardium near the junction of the superior vena cava and the right atrium. After implantation, the dialysis probe was perfused with Ringer's solution (in mmol/L: NaCl 147, KCl 4, $CaCl_2$ 3) containing a cholinesterase inhibitor eserine (100 μmol/L), at a speed of 2 μl/min using a microinjection pump (CMA/102, Carnegie Medicin, Sweden). Experimental protocols were started 120 min after implantation of the dialysis probe. The dead space between the dialysis membrane and the sample tube was taken into account at the beginning of each dialysate sampling. In protocols 1 and 2 as described below, 8 μl of phosphate buffer (pH 3.5) was added to each sample tube before dialysate sampling, and each dialysate sampling period was set at 20 min (1 sample volume=40 μl). Half of the dialysate sample was used for ACh and the other half for NE measurements. In protocol 3, 2 μl of phosphate buffer was added to each sample tube before dialysate sampling, and each dialysate sampling period was set at 5 min (1 sample volume=10 μl). In protocol 4, 4 μl of phosphate buffer was added to each sample tube before dialysate sampling, and each dialysate sampling period was set at 10 min (1 sample volume=20 μl). Dialysate NE and ACh concentrations were analyzed separately by high-performance liquid chromatography as described previously.[12,13]

Experimental Protocols

Protocol 1 (n=7) Baseline dialysate was sampled before the injection of medetomidine. Thereafter, a low dose (10 μg/kg) of medetomidine was injected intravenously via the femoral vein. After allowing 20 min for hemodynamic stabilization, dialysate was sampled for 20 min (40 μl). When the hemodynamics had recovered to the baseline level, a high dose (100 μg/kg) of medetomidine was injected intravenously and another 20-min dialysate sample was collected after hemodynamic stabilization. Finally, the vagal nerves were sectioned bilaterally at the neck and a dialysate sample was collected immediately after vagotomy. In 4 rabbits, an α_2-adrenergic antagonist, atipamezole (2.5 mg/kg), was intravenously administered before euthanasia and hemodynamic responses were recorded.

Protocol 2 (n=7) To prevent possible interference of medetomidine-induced hypotension with vagal nerve activity, intravenous infusion of an α_1-adrenergic agonist, phenylephrine, was started simultaneous to intravenous injection of medetomidine. Baseline dialysate sample was collected for 20 min before medetomidine injection. Simultaneous to intravenous injection of high-dose (100 μg/kg) medetomidine, intravenous infusion of phenylephrine was started (6.6±1.2 μg·kg^{-1}·min^{-1}) to maintain the mean blood pressure (BP) at baseline level. After hemodynamic stabilization, dialysate was sampled for 20 min. Finally, dialysate was again sampled immediately after bilateral cervical vagotomy.

Protocol 3 To investigate the effect of medetomidine on baroreflex-induced vagal ACh release, we varied the mean BP by changing the dose of intravenous phenylephrine in both the control (n=5) and medetomidine-treated (n=7) groups. In the control group, Ringer's solution was infused intravenously at 1.0 ml·kg^{-1}·h^{-1} throughout the experiment. In the medetomidine-treated group, medetomidine was initially injected intravenously at a dose of 60 μg/kg, and thereafter continuously infused at a dose of 60 μg·kg^{-1}·h^{-1} or a rate of 1.0 ml·kg^{-1}·h^{-1}. After baseline dialysate sampling, mean BP was increased in a stepwise manner by altering the dose of intravenous phenylephrine (maximal dose: 32.2±5.5 μg·kg^{-1}·min^{-1} in the control group and 18.6±2.1 μg·kg^{-1}·min^{-1} in the medetomidine-treated group). Dialysate samples were collected for 5 min at 4–7 different mean BP levels. Relations of log ACh concentrations vs. mean BP were plotted and regression lines for each animal were calculated.

Protocol 4 (n=5) We investigated the peripheral effects of medetomidine on heart rate and dialysate ACh concentration under electrical stimulation of the right cervical vagal nerve. Bilateral vagal nerves were exposed through a midline cervical incision and sectioned at the neck. A pair of bipolar stainless steel electrodes was attached to the efferent side of the

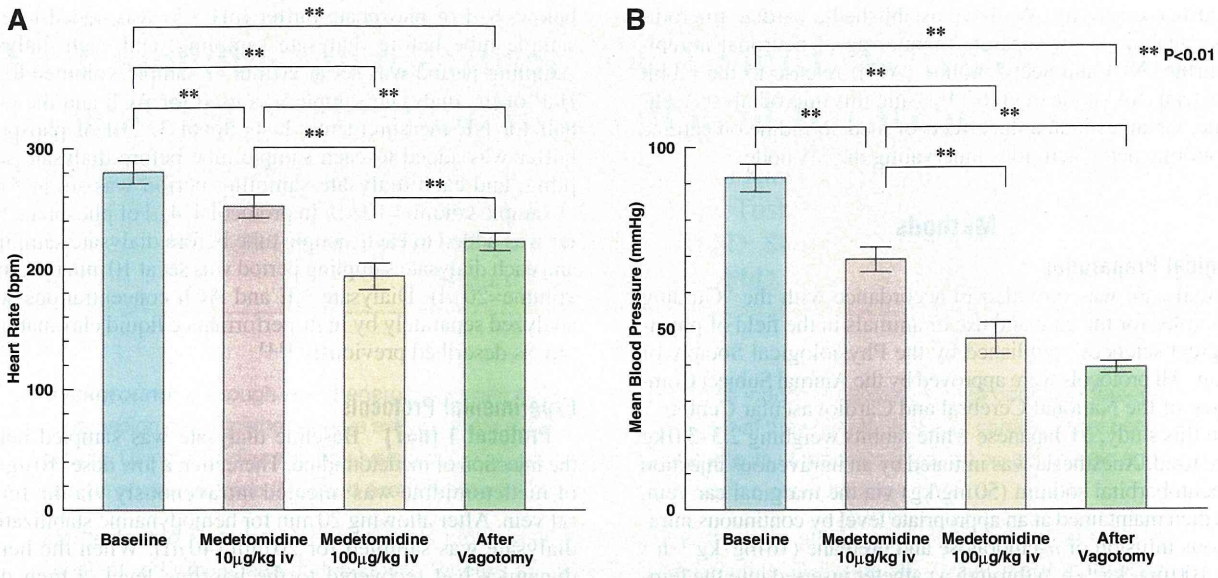

Figure 1. Intravenous administration of low and high doses of medetomidine decreased heart rate (**A**) and mean blood pressure (**B**). Medetomidine decreased heart rate in a dose-dependent manner. Vagotomy partially restored the decrease in heart rate but had no effect on mean blood pressure under administration of 100 μg/kg of medetomidine. **P<0.01.

right vagal nerve. The nerve and electrode were covered with warmed mineral oil for insulation. After the baseline dialysate sampling, the right efferent vagal nerve was stimulated at the frequency of 20 Hz by a digital stimulator (SEN-7203, Nihon Kohden, Japan). The pulse duration and amplitude of nerve stimulation were set at 1 ms and 10 V. Thereafter, a low dose (10 μg/kg) of medetomidine was injected intravenously via the femoral vein. After hemodynamic stabilization, dialysate was sampled for 10 min under the 20-Hz electrical stimulation of vagal nerve. Finally, a high dose (100 μg/kg) of medetomidine was injected intravenously and another 10-min dialysate sample was collected under the 20-Hz electrical stimulation.

Statistical Analysis

All data are presented as mean±standard error. Heart rate and mean BP were compared by 1-way repeated measures analysis of variance (ANOVA) followed by a Tukey's test.[14] Dialysate NE and ACh concentrations were also compared by 1-way repeated measures ANOVA followed by a Tukey's test. Comparisons of data between protocols 1 and 2 were conducted using unpaired t-test (Student's or Welch's t-test). In protocol 3, the average slopes and intercepts of the regression lines were compared using unpaired t-test. Differences were considered significant at P<0.05.

Results

Protocol 1

Intravenous injection of medetomidine significantly decreased heart rate (**Figure 1A**) and mean BP (**Figure 1B**) in a dose-dependent manner (280±10 beats/min and 92±4 mmHg, respectively, at baseline; 251±10 beats/min and 69±3 mmHg at 10 μg/kg; and 193±11 beats/min and 47±4 mmHg at 100 μg/kg, P<0.01 for all comparisons). Vagotomy increased heart rate to 222±7 beats/min but did not affect mean BP (**Figures 1A,B**).

Low-dose medetomidine significantly decreased dialysate NE concentration (**Figure 2A**) from 0.72±0.06 to 0.59±0.04 nmol/L (P<0.01) but did not affect dialysate ACh concentration (**Figure 2B**) compared with baseline. High-dose medetomidine also decreased dialysate NE concentration (to 0.52±0.05 nmol/L) similar to low-dose medetomidine (**Figure 2A**) and significantly increased dialysate ACh concentration from 7.2±1.3 nmol/L at baseline to 12.1±1.6 nmol/L (P<0.01, **Figure 2B**). Dialysate NE concentration was not changed by vagotomy, whereas dialysate ACh concentration recovered to the baseline level immediately after vagotomy (**Figures 2A,B**).

In 4 rabbits treated with atipamezole, heart rate and mean BP recovered to the baseline levels immediately after the injection (276±18 beats/min and 88±6 mmHg, respectively, at baseline; and 280±11 beats/min and 83±6 mmHg after the injection).

Protocol 2

Intravenous injection of high-dose medetomidine combined with phenylephrine decreased heart rate (**Figure 3A**) and the decrease was significantly greater than that observed in protocol 1 (140±9 vs. 193±11 beats/min, P<0.01), while mean BP was maintained at the same level as baseline (**Figure 3B**). Medetomidine combined with phenylephrine decreased dialysate NE concentration from 0.85±0.09 at baseline to 0.68±0.10 nmol/L (**Figure 4A**), and the decrease was not significantly different from that of medetomidine alone (protocol 1). However, medetomidine combined with phenylephrine increased dialysate ACh concentration (**Figure 4B**) to a significantly and markedly higher level than that observed in protocol 1 (26.8±5.4 vs. 12.1±1.6 nmol/L, P<0.05). Dialysate ACh concentration recovered to the baseline level immediately after vagotomy.

Protocol 3

The change in mean BP by phenylephrine administration affected dialysate ACh concentration only slightly in the control group (**Figure 5A**), whereas the elevation of mean BP

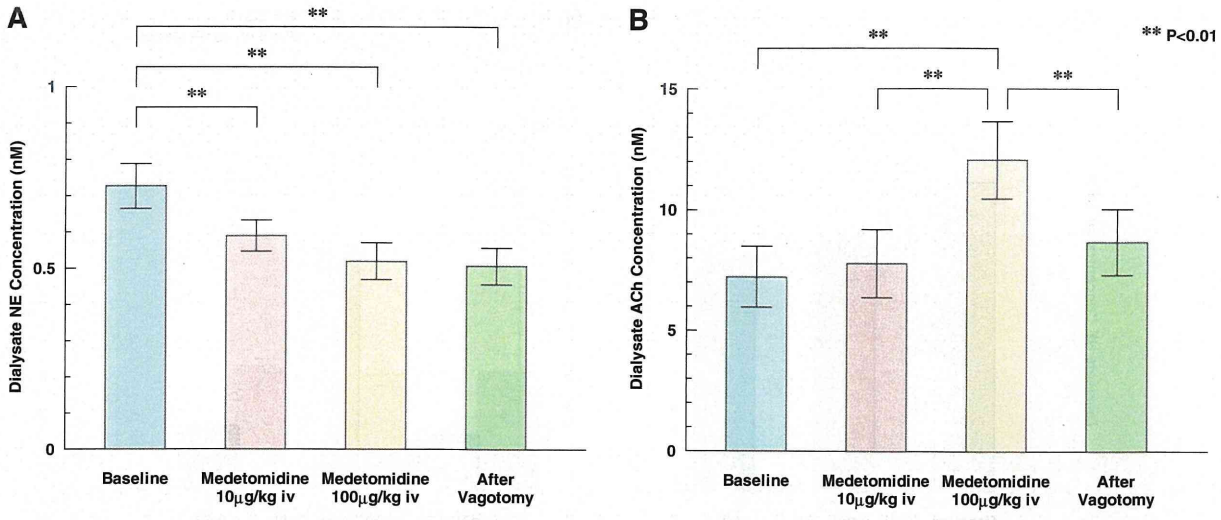

Figure 2. Effects of intravenous administration of low and high doses of medetomidine on dialysate NE (**A**) and ACh concentrations (**B**). Medetomidine at 10 and 100 μg/kg similarly decreased dialysate NE concentration (**A**). Medetomidine at 100 μg/kg significantly increased dialysate ACh concentration, but 10 μg/kg had no effect (**B**). Vagotomy suppressed the increase in dialysate ACh concentration. **P<0.01. ACh, acetylcholine; NE, norepinephrine.

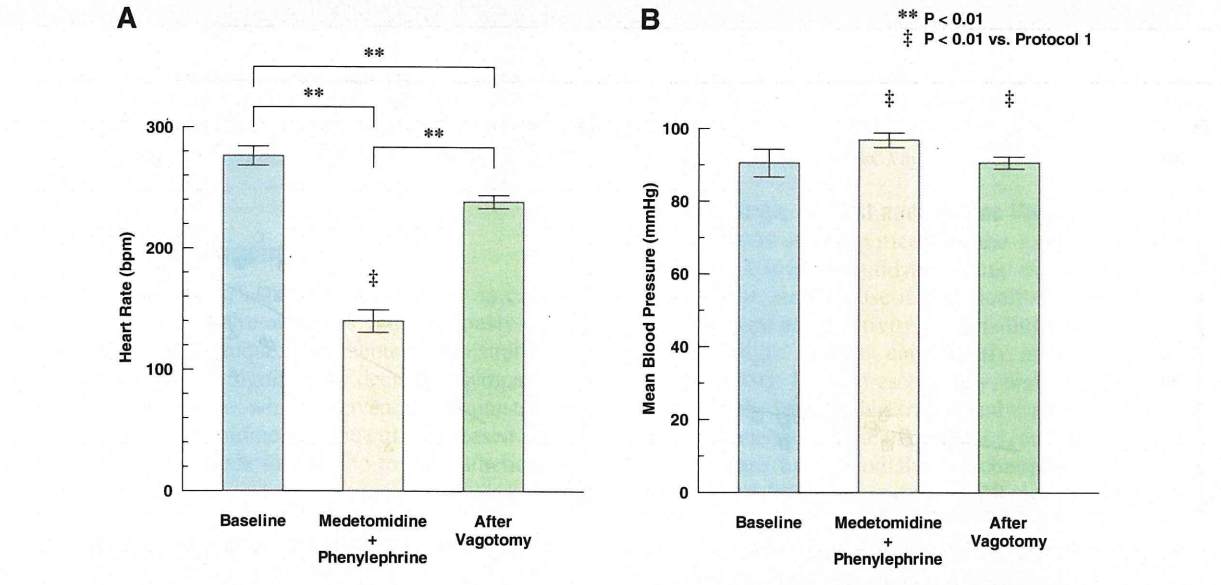

Figure 3. Effects of simultaneous intravenous administration of medetomidine and phenylephrine on heart rate (**A**) and mean blood pressure (**B**). Medetomidine combined with phenylephrine significantly decreased heart rate (**A**), and the decrease was significantly greater compared with medetomidine alone (protocol 1: **Figure 1A**). Medetomidine combined with phenylephrine maintained mean blood pressure (**B**) at the baseline level. Vagotomy partially restored the decrease in heart rate but had no effect on mean blood pressure. **P<0.01; ‡P<0.01 vs. medetomidine alone (protocol 1: **Figure 1A**).

markedly increased dialysate ACh concentration in the medetomidine-treated group (**Figure 5B**). The average slopes of the regression lines between mean BP and log dialysate ACh concentration were 0.0018±0.0004 in the control and 0.0062±0.0006 in the medetomidine-treated group. The slope was significantly steeper in the medetomidine-treated group than that in the control (P<0.01). However, the intercept did not differ significantly between the control (0.59±0.05) and medetomidine-treated (0.68±0.07) groups.

Protocol 4

The 20-Hz electrical stimulation of the right vagal nerve significantly decreased heart rate from 271±11 beats/min at the baseline to 112±6 beats/min and increased dialysate ACh concentration from 7.1±0.9 nmol/L at the baseline to 38.5±7.2 nmol/L (P<0.01). However, both 10 and 100 μg/kg of me-

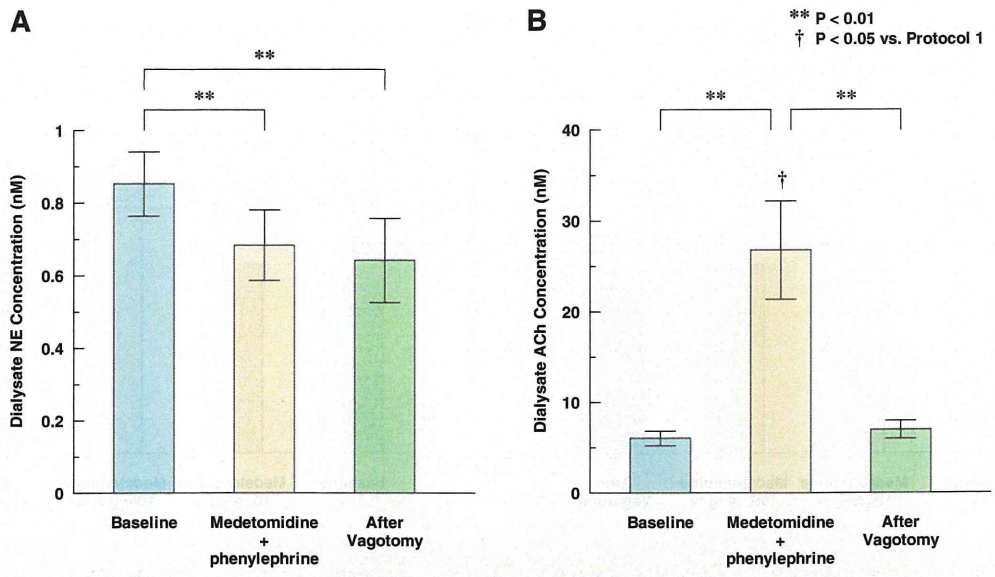

Figure 4. Effects of simultaneous intravenous administration of medetomidine and phenylephrine on dialysate NE (**A**) and ACh concentrations (**B**). Medetomidine combined with phenylephrine decreased dialysate NE concentration (**A**), and the decrease was similar to medetomidine alone (protocol 1: **Figure 2A**). Medetomidine combined with phenylephrine caused a marked increase in dialysate ACh concentration (**B**) and the increase was significantly greater than medetomidine alone (protocol 1: **Figure 2B**). Vagotomy suppressed the increase in dialysate ACh concentration. **P<0.01; †P<0.05 vs. medetomidine alone (protocol 1: **Figure 2B**). ACh, acetylcholine; NE, norepinephrine.

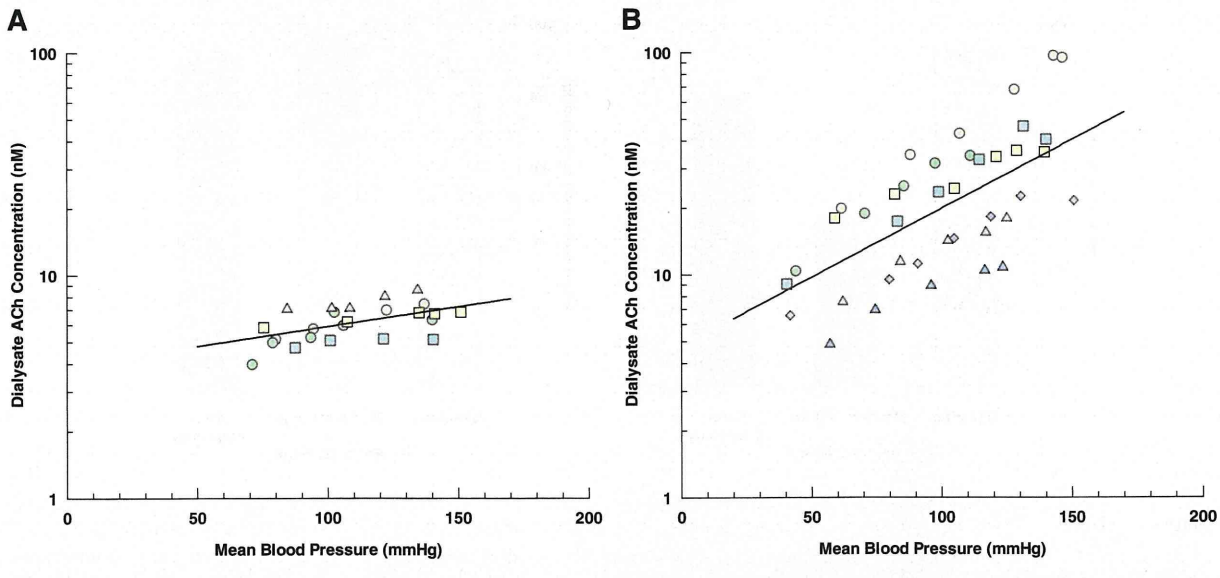

Figure 5. Regression lines of dialysate ACh concentration vs. MBP in control group (**A**) and medetomidine-treated group (**B**). In the control group (n=5), the increase in MBP had little effect on dialysate ACh concentration (**A**). In the medetomidine-treated group (n=7), dialysate ACh concentration was elevated with increase in MBP (**B**). Average regression line for control group: log[ACh]= 0.0018×MBP+0.59. Average regression line for medetomidine-treated group: log[ACh]=0.0062×MBP+0.68. Each symbol represents the data of 1 animal. ACh, acetylcholine; MBP, mean blood pressure.

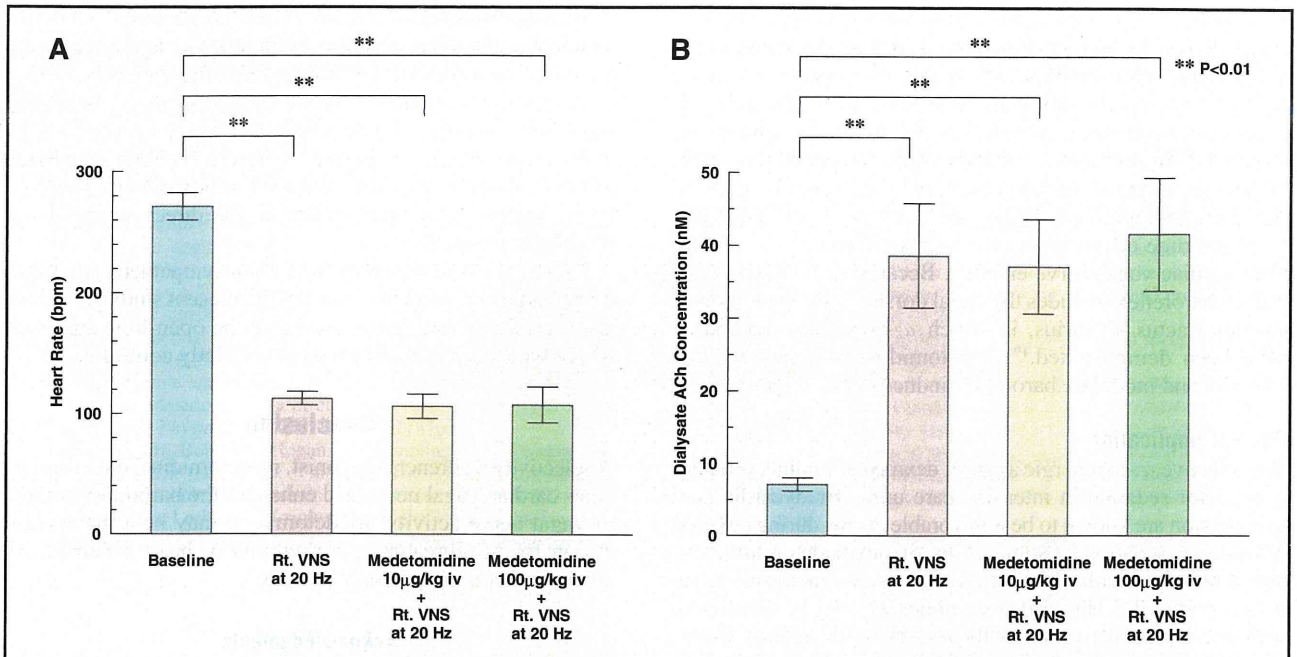

Figure 6. Peripheral effects of medetomidine on heart rate (**A**) and dialysate acetylcholine (ACh) concentration (**B**) under electrical stimulation of the right cervical vagal nerve. The 20-Hz electrical stimulation of the right cervical vagal nerve significantly decreased heart rate and increased dialysate ACh concentration. However, medetomidine did not affect the heart rate and dialysate ACh concentration under electrical vagal nerve stimulation (VNS).

detomidine did not affect heart rate and dialysate ACh concentration under the electrical stimulation (106±9.9 beats/min and 37.1±6.1 nmol/L at 10 μg/kg, 108±15 beats/min and 41.6±7.7 nmol/L at 100 μg/kg).

Discussion

We have elucidated the effects of medetomidine on cardiac sympathetic and vagal nerve activities simultaneously using cardiac microdialysis technique. Intravenous administration of 10 μg/kg of medetomidine significantly decreased sympathetic NE release to the SA node, while intravenous administration of 100 μg/kg of medetomidine significantly increased vagal ACh release to the SA node in addition to sympathetic suppression.

α2-Adrenergic Agonist and Cardiac Sympathetic Nerve Activity

It is well-documented that α2-adrenergic agonist suppresses sympathetic nerve activity.[15] Oku et al reported that dexmedetomidine suppressed renal sympathetic nerve discharge in baroreceptor-denervated rabbits.[16] In the present study, low-dose medetomidine decreased heart rate and mean BP through inhibiting sympathetic nerve activity, without affecting cardiac vagal nerve activity. High-dose medetomidine also suppressed NE release to the same level as low-dose medetomidine.

Several mechanisms may be involved in the sympathoinhibitory effect of α2-adrenergic agonist. The rostral ventrolateral medulla has been reported to serve as an important site in mediating the hypotensive and sedative effects of α2-adrenergic agonist.[17] McCallum et al reported that the central sympathoinhibitory effects of α2-adrenoceptor stimulation are augmented by peripheral inhibition of ganglionic transmission.[18] The results obtained from protocol 1 indicate that low-dose medetomidine may induce a vagal-dominant condition through suppression of the cardiac sympathetic nerve without direct activation of the cardiac vagal nerve.

α2-Adrenergic Agonist and Cardiac Vagal Nerve Activity

Kamibayashi et al reported that the vagus nerve played an important role in the antidysrhythmic effect of dexmedetomidine.[3] However, because it is difficult to selectively monitor cardiac vagal nerve activity, there is little direct evidence that α2-adrenergic agonists can directly increase cardiac vagal nerve activity. In the present study, high-dose medetomidine significantly decreased heart rate and mean BP compared with low-dose medetomidine in protocol 1, and analyses of NE and ACh release by microdialysis technique proved that these decreases in heart rate and mean BP were associated with an increase in vagal ACh release to the heart. Histocytological studies demonstrated the presence of α2-adrenergic receptors in the vagal dorsal motor nucleus and nucleus tractus solitarius.[19] Therefore, it is possible that α2-adrenergic agonists directly activate the cardiac vagal nerve. It is also possible that intravenous medetomidine also modulates vagal ACh release through ganglionic transmission and the direct action to nerve endings. In protocol 4, however, medetomidine did not affect heart rate or the dialysate ACh concentration under electrical stimulation of the right efferent vagal nerve. Thus, in our experimental setting the peripheral effects of medetomidine on cardiac vagal nerve activity may be small compared with its central effects.

To exclude the possibility that medetomidine-induced hypotension affects local ACh concentrations, the mean BP was maintained constant by co-administration of phenylephrine in protocol 2. High-dose medetomidine combined with phenylephrine enhanced the decrease in heart rate and the increase in dialysate ACh concentration without medetomi-

dine-induced hypotension, indicating that hypotension occurring in protocol 1 had actually reduced ACh release in response to high-dose medetomidine. The results also suggest an interaction between baroreflex-induced and medetomidine-induced vagal nerve activation, which was extensively examined in protocol 3. In protocol 3, medetomidine steepened the slope of the regression line between mean BP and log dialysate ACh concentration, without affecting the intercept. In other words, medetomidine enhanced the baroreflex-induced ACh release from cardiac vagal nerve endings. Because the central pathway of baroreflex includes the vagal dorsal motor nucleus and nucleus tractus solitarius, in which α_2-adrenergic receptors have been demonstrated,[19] medetomidine may act on this pathway and modulate baroreflex-induced ACh release.

Clinical Implication

The selective α_2-adrenergic agonist, dexmedetomidine, is widely used for sedation in intensive care units. Bradycardia and hypotension are known to be unfavorable events during dexmedetomidine sedation.[20] Some cases of dexmedetomidine-induced atrioventricular block followed by cardiac arrest have been reported.[21,22] This critical complication may be associated with direct vagal activation by the α_2-adrenergic agonist. Compared with our previous results of electrical cervical vagal nerve stimulation in rabbits,[9] intravenous administration of 100 μg/kg of medetomidine had an effect equivalent to electrical vagal stimulation at 10 Hz. Furthermore, when the mean BP was maintained constant using phenylephrine, medetomidine had a stronger effect on cardiac vagal nerve activity, which is similar to 20-Hz electrical vagal stimulation, and this magnitude may sometimes cause atrioventricular block or sinus arrest.

Notwithstanding these adverse effects, vagal activation has several favorable cardioprotective effects. Our study proved that medetomidine, a selective α_2-adrenergic agonist, is a strong activator of cardiac vagal nerve. Vanoli et al[6] reported that vagal stimulation after acute ischemia can prevent ventricular fibrillation. Ando et al reported that efferent vagal nerve stimulation prevented ischemia-induced arrhythmias by preserving connexin 43 protein.[23] Our results suggest that vagal activation in addition to sympathetic suppression probably contributes to the antiarrhythmic effect of medetomidine.

Because inhibition of the sympathetic nerve system has been the cornerstone of drug therapy for heart failure,[24] a selective α_2-adrenergic agonist may be a potential therapeutic option for heart failure. Recent studies have shown that electrical vagal nerve stimulation also improves the outcomes in patients with heart failure.[25] Electrical stimulation of carotid baroreceptor has recently been reported to be a therapeutic option for heart failure. Sabbah et al reported that chronic electrical stimulation of the carotid sinus baroreflex improved left ventricular function and promoted reversal of ventricular remodeling in dogs with advanced heart failure.[26] Our study demonstrated that medetomidine modulates baroreflex control to enhance vagal nerve activity, which may also induce further cardioprotective effects.

Study Limitations

First, ACh is degraded by ACh esterase immediately after release. Therefore, detection of in vivo ACh release requires the addition of eserine, a specific ACh esterase inhibitor, into the perfusate. The presence of eserine around the semipermeable membrane might have affected ACh release in the vicinity of the semipermeable membrane. Eserine could have activated regulatory pathways such as autoinhibition of ACh release via muscarinic receptors.

Second, medetomidine is a chiral imidazole derivative. Thus, imidazoline receptors may also be involved in the cardiac vagal activation by medetomidine. Further investigation is necessary to clarify the influence of imidazoline receptors on cardiac vagal nerve activity. However, because an α_2-adrenergic antagonist, atipamezole, abolished the hemodynamic responses to medetomidine, we think that the cardiovascular effects of medetomidine are mainly related to the direct action of α_2-adrenergic receptors.

Third, the interactive effects between sympathetic and vagal nerve endings remain uncertain in the present study. Thus, we need further investigations including the open-loop approach where baroreceptor input pressure is strictly controlled.

Conclusion

A selective α_2-adrenergic agonist, medetomidine, directly activates cardiac vagal nerve and enhances the baroreflex control of vagal nerve activity. Medetomidine may be a therapeutic option for life-threatening arrhythmia or heart failure if the adverse effects are properly managed.

Acknowledgments

This study was supported by a research project promoted by the Japanese Ministry of Health, Labour and Welfare (H20-katsudo-Shitei-007 and H21-nano-Ippan-005); Grants-in-Aid for Scientific Research (No. 20390462 and No. 23592319) from the Ministry of Education, Culture, Sports, Science and Technology; the Industrial Technology Research Grant Program from New Energy and Industrial Technology Development Organization (NEDO) of Japan; and Dr Hiroshi Irisawa & Dr Aya Irisawa Memorial Research Grant from the Japan Heart Foundation.

References

1. Hsu YW, Cortinez LI, Robertson KM, Keifer JC, Sum-Ping ST, Moretti EW, et al. Dexmedetomidine pharmacodynamics: Part I: Crossover comparison of the respiratory effects of dexmedetomidine and remifentanil in healthy volunteers. *Anesthesiology* 2004; **101:** 1066–1076.
2. Hayashi Y, Sumikawa K, Maze M, Yamatodani A, Kamibayashi T, Kuro M, et al. Dexmedetomidine prevents epinephrine-induced arrhythmias through stimulation of central alpha 2 adrenoceptors in halothane-anesthetized dogs. *Anesthesiology* 1991; **75:** 113–117.
3. Kamibayashi T, Hayashi Y, Mammoto T, Yamatodani A, Sumikawa K, Yoshiya I. Role of the vagus nerve in the antidysrhythmic effect of dexmedetomidine on halothane/epinephrine dysrhythmias in dogs. *Anesthesiology* 1995; **83:** 992–999.
4. Yamazaki T, Asanoi H, Ueno H, Yamada K, Takagawa J, Kameyama T, et al. Central sympathetic inhibition augments sleep-related ultradian rhythm of parasympathetic tone in patients with chronic heart failure. *Circ J* 2005; **69:** 1052–1056.
5. Lombardi F, Sandrone G, Pernpruner S, Sala R, Garimoldi M, Cerutti S, et al. Heart rate variability as an index of sympathovagal interaction after acute myocardial infarction. *Am J Cardiol* 1987; **60:** 1239–1245.
6. Vanoli E, De Ferrari GM, Stramba-Badiale M, Hull SS Jr, Foreman RD, Schwartz PJ. Vagal stimulation and prevention of sudden death in conscious dogs with a healed myocardial infarction. *Circ Res* 1991; **68:** 1471–1481.
7. Schwartz PJ, La Rovere MT, Vanoli E. Autonomic nervous system and sudden cardiac death: Experimental basis and clinical observations for post-myocardial infarction risk stratification. *Circulation* 1992; **85:** I77–I91.
8. Kuusela E, Raekallio M, Anttila M, Falck I, Mölsä S, Vainio O. Clinical effects and pharmacokinetics of medetomidine and its enantiomers in dogs. *J Vet Pharmacol Ther* 2000; **23:** 15–20.
9. Shimizu S, Akiyama T, Kawada T, Shishido T, Yamazaki T, Kamiya A, et al. In vivo direct monitoring of vagal acetylcholine release to the sinoatrial node. *Auton Neurosci* 2009; **148:** 44–49.
10. Shimizu S, Akiyama T, Kawada T, Shishido T, Mizuno M, Kamiya A, et al. In vivo direct monitoring of interstitial norepinephrine levels at the sinoatrial node. *Auton Neurosci* 2010; **152:** 115–118.
11. Shimizu S, Akiyama T, Kawada T, Sonobe T, Kamiya A, Shishido T, et al. Centrally administered ghrelin activates cardiac vagal nerve

in anesthetized rabbits. *Auton Neurosci* 2011; **162:** 60–65.
12. Akiyama T, Yamazaki T, Ninomiya I. In vivo monitoring of myocardial interstitial norepinephrine by dialysis technique. *Am J Physiol* 1991; **261:** H1643–H1647.
13. Akiyama T, Yamazaki T, Ninomiya I. In vivo detection of endogenous acetylcholine release in cat ventricles. *Am J Physiol* 1994; **266:** H854–H860.
14. Glantz SA. Primer of biostatistics. 6th edn. New York: McGraw-Hill, 2005.
15. Heusch G, Schipke J, Thämer V. Clonidine prevents the sympathetic initiation and aggravation of poststenotic myocardial ischemia. *J Cardiovasc Pharmacol* 1985; **7:** 1176–1182.
16. Oku S, Benson KT, Hirakawa M, Goto H. Renal sympathetic nerve activity after dexmedetomidine in nerve-intact and baroreceptor-denervated rabbits. *Anesth Analg* 1996; **83:** 477–481.
17. Yamazato M, Sakima A, Nakazato J, Sesoko S, Muratani H, Fukiyama K. Hypotensive and sedative effects of clonidine injected into the rostral ventrolateral medulla of conscious rats. *Am J Physiol Regul Integr Comp Physiol* 2001; **281:** R1868–R1876.
18. McCallum JB, Boban N, Hogan Q, Schmeling WT, Kampine JP, Bosnjak ZJ. The mechanism of alpha2-adrenergic inhibition of sympathetic ganglionic transmission. *Anesth Analg* 1998; **87:** 503–510.
19. Robertson HA, Leslie RA. Noradrenergic alpha 2 binding sites in vagal dorsal motor nucleus and nucleus tractus solitarius: Autoradiographic localization. *Can J Physiol Pharmacol* 1985; **63:** 1190–1194.
20. Candiotti KA, Bergese SD, Bokesch PM, Feldman MA, Wisemandle W, Bekker AY; MAC Study Group. Monitored anesthesia care with dexmedetomidine: A prospective, randomized, double-blind, multicenter trial. *Anesth Analg* 2010; **110:** 47–56.
21. Nagasaka Y, Machino A, Fujikake K, Kawamoto E, Wakamatsu M. Cardiac arrest induced by dexmedetomidine. *Masui* 2009; **58:** 987–989.
22. Ingersoll-Weng E, Manecke GR Jr, Thistlethwaite PA. Dexmedetomidine and cardiac arrest. *Anesthesiology* 2004; **100:** 738–739.
23. Ando M, Katare RG, Kakinuma Y, Zhang D, Yamasaki F, Muramoto K, et al. Efferent vagal nerve stimulation protects heart against ischemia-induced arrhythmias by preserving connexin43 protein. *Circulation* 2005; **112:** 164–170.
24. Sata Y, Krum H. The future of pharmacological therapy for heart failure. *Circ J* 2010; **74:** 809–817.
25. Schwartz PJ. Vagal stimulation for heart diseases: From animals to men: An example of translational cardiology. *Circ J* 2010; **75:** 20–27.
26. Sabbah HN, Gupta RC, Imai M, Irwin ED, Rastogi S, Rossing MA, et al. Chronic electrical stimulation of the carotid sinus baroreflex improves left ventricular function and promotes reversal of ventricular remodeling in dogs with advanced heart failure. *Circ Heart Fail* 2011; **4:** 65–70.

Life Sciences 89 (2011) 498–503

Contents lists available at ScienceDirect

Life Sciences

journal homepage: www.elsevier.com/locate/lifescie

Contrasting effects of moderate vagal stimulation on heart rate and carotid sinus baroreflex-mediated sympathetic arterial pressure regulation in rats

Toru Kawada [a,*], Shuji Shimizu [a], Meihua Li [a], Atsunori Kamiya [a], Kazunori Uemura [a], Yusuke Sata [a], Hiromi Yamamoto [b], Masaru Sugimachi [a]

[a] Department of Cardiovascular Dynamics, National Cerebral and Cardiovascular Center Research Institute, Osaka 565-8565, Japan
[b] Division of Cardiology, Department of Internal Medicine, Kinki University School of Medicine, Osaka 589-8511, Japan

ARTICLE INFO

Article history:
Received 30 March 2011
Accepted 19 July 2011

Keywords:
Carotid sinus baroreflex
Open-loop analysis
Sympathetic nerve activity

ABSTRACT

Aims: To examine whether moderate efferent vagal nerve stimulation (VNS) attenuates the carotid sinus baroreflex-mediated arterial pressure (AP) regulation via its antagonism to the sympathetic system.
Main methods: Carotid sinus baroreceptor regions were isolated from the systemic circulation in eight anesthetized and vagotomized rats. A staircase-wise input was imposed on carotid sinus pressure (CSP) with or without efferent VNS (20 Hz, 2 ms, 1–4 V), while the responses in AP, heart rate (HR), and splanchnic sympathetic nerve activity (SNA) were measured.
Key findings: A multiple linear regression analysis indicated that VNS decreased the minimum HR in the CSP–HR relationship by 58.2 ± 4.9 beats/min ($P<0.01$) from its reference value of 387.0 ± 5.8 beats/min. Although VNS significantly decreased an intercept of the SNA–AP relationship, it did not affect parameters of the CSP–AP relationship or the CSP–SNA relationship significantly. The operating-point AP of the baroreflex was decreased by 2.8 ± 1.0 mm Hg ($P<0.01$) during VNS, which was less than 3% of the reference value of 117.7 ± 1.2 mm Hg.
Significance: VNS, at an intensity of decreasing HR by approximately 13%, does not acutely attenuate the baroreflex-mediated sympathetic AP regulation.

Introduction

Vagal nerve stimulation (VNS) has been proposed as a new therapeutic approach to improve long-term survival of chronic heart failure in rats (Li et al., 2004). The feasibility of VNS in chronic heart failure patients has been reported (De Ferrari et al., 2011; Schwartz, 2010). Because excess sympathetic activity has deleterious effects on the failing heart, VNS is considered to provide beneficial effects through its antagonism to the sympathetic system. On the other hand, if VNS significantly attenuates the sympathetic arterial pressure (AP) regulation through the antagonism to the sympathetic system, resulting adverse effects such as reduced orthostatic tolerance may limit the utility of VNS. In fact, VNS can cause bradycardia and hypotension depending on the intensity of stimulation (Shimizu et al., 2009). The effect of VNS on the sympathetic AP regulation, however, is not fully understood, partially because the arterial baroreflex always buffers changes in AP and obscures the pure VNS effect on AP. Another concern is that the magnitude of VNS-induced antagonism to the sympathetic system could vary depending on the level of sympathetic nerve activity (SNA). To elucidate the pure effect of VNS on the sympathetic AP regulation at various levels of SNA, a baroreflex open-loop analysis described below is required.

The sympathetic arterial baroreflex can be divided into two principal subsystems: a neural arc subsystem from pressure input to efferent SNA, and a peripheral arc subsystem from SNA to AP (Mohrman and Heller, 2006; Ikeda et al., 1996; Sato et al., 1999a, 1999b). Under normal physiological conditions, AP affects SNA through the neural arc, while SNA in turn affects AP through the peripheral arc. This closed-loop operation makes it difficult to identify the input–output relationships of the two arcs separately (Kawada et al., 1997; Kamiya et al., 2011). To circumvent the problem, a baroreflex open-loop analysis using an isolated carotid sinus preparation has been employed (Kawada et al., 2009, 2010). In the present study, a hypothesis that moderate efferent VNS attenuates the baroreflex-mediated sympathetic AP regulation was tested in anesthetized and vagotomized rats.

Materials and methods

Surgical preparation

Animal care was provided in strict accordance with the *Guiding Principles for the Care and Use of Animals in the Field of Physiological Sciences*, approved by the Physiological Society of Japan. All protocols were reviewed and approved by the Animal Subject Committee of National Cerebral and Cardiovascular Center. Eight male Sprague–

* Corresponding author at: Department of Cardiovascular Dynamics, National Cerebral and Cardiovascular Center Research Institute, 5-7-1 Fujishirodai, Suita, Osaka 565-8565, Japan. Tel.: +81 6 6833 5012x2427; fax: +81 6 6835 5403.
E-mail address: torukawa@res.ncvc.go.jp (T. Kawada).

0024-3205/$ – see front matter © 2011 Elsevier Inc. All rights reserved.
doi:10.1016/j.lfs.2011.07.026

Dawley rats (408–590 g) were anesthetized by an intraperitoneal injection (2 ml/kg) of a mixture of α-chloralose (40 mg/ml) and urethane (250 mg/ml), and ventilated mechanically with oxygen-supplied room air. The depth of anesthesia was maintained with a 20-fold diluted solution of the above anesthetic mixture infused from the right femoral vein (2–3 ml kg^{-1} h^{-1}). Another venous catheter was inserted into the left femoral vein to supply Ringer solution (6 ml kg^{-1} h^{-1}). AP was measured from a catheter inserted into the right femoral artery. Heart rate (HR) was detected from AP using a cardiotachometer (AT-601G, Nihon Kohden, Tokyo, Japan). Body temperature of the animal was maintained by a heating pad at approximately 38 °C.

A postganglionic branch of the splanchnic sympathetic nerve was exposed through a left flank incision. A pair of stainless steel wire electrodes (Bioflex wire, AS633, Cooner Wire, CA, USA) was attached to the nerve to record SNA. The nerve and electrodes were secured and insulated with silicone glue (Kwik-Sil, World Precision Instruments, FL, USA). To quantify SNA, a preamplified nerve signal was band-pass filtered at 150–1000 Hz, and then full-wave rectified and low-pass filtered with a cut-off frequency of 30 Hz using analog circuits. Pancuronium bromide (0.4 mg kg^{-1} h^{-1}) was given continuously to prevent muscular activity from contaminating SNA. At the end of the experiment, a bolus injection of a ganglionic blocker hexamethonium bromide (60 mg/kg) was given to confirm the disappearance of SNA and to measure the noise level.

Carotid sinus baroreceptor regions were isolated from the systemic circulation according to previously reported procedures (Shoukas et al., 1991; Sato et al., 1999a, 1999b) with modifications. Briefly, a 7–0 polypropylene suture with a fine needle (PROLENE, Ethicon, GA, USA) was passed through the tissue between the external and internal carotid arteries, and the external carotid artery was ligated close to the carotid bifurcation. The internal carotid artery was embolized with two to three steel balls (0.8 mm in diameter, Tsubaki Nakashima, Nara, Japan) injected from the common carotid artery. The isolated carotid sinuses were filled with Ringer solution through catheters inserted into the common carotid arteries. Carotid sinus pressure (CSP) was controlled using a servo-controlled piston pump. Heparin sodium (100 U/kg) was given intravenously to prevent blood coagulation.

Bilateral vagal and aortic depressor nerves were sectioned at the neck to avoid reflexes from the cardiopulmonary region and aortic arch. A pair of stainless steel wire electrodes (Bioflex wire, AS633, Cooner Wire, CA, USA) was attached to the sectioned right vagus for efferent VNS. The nerve and electrodes were secured and insulated with silicone glue (Kwik-Sil, World Precision Instruments, FL, USA).

Protocol

After the surgical procedures were completed, responses in SNA, AP, and HR to a CSP input were monitored for more than 30 min. The rat was excluded from the study if the reflex responses became smaller within this stabilization period. Possible causes for the deterioration of the baroreflex responses include surgical damage to the carotid sinus nerves and brain ischemia due to bilateral carotid occlusion. After the stabilization period, CSP was matched to instantaneous AP to make the carotid sinus baroreflex virtually closed, and baseline hemodynamic data were recorded for 10 min.

To estimate open-loop static input–output relationship of the carotid sinus baroreflex, CSP was first decreased to 60 mm Hg for 4 min. CSP was then increased from 60 to 180 mm Hg every minute in increments of 20 mm Hg (Kawada et al., 2009, 2010). The staircase-wise input cycle was repeated throughout the protocol. VNS was applied to the right vagus at 20 Hz with a pulse duration of 2 ms. The square pulse with this pulse duration was not intended to mimic naturally occurring vagal nerve activity; rather, the stimulation parameters were determined based on a previous study showing that VNS with this setting can produce significant bradycardia (Mizuno et al., 2011). The amplitude of VNS was adjusted (1–4 V) in each animal to reduce HR by approximately 50 beats/min before starting the staircase-wise input protocol. Data were recorded for two cycles before VNS, three cycles during VNS, and two cycles after VNS.

Data analysis

Data were sampled at 200 Hz using a 16-bit analog-to-digital converter and stored on a dedicated laboratory computer system. There was a transient response after changing the level of CSP. To estimate the input–output relationship at the steady state, mean AP, HR, and SNA were calculated during the last 10 s at each CSP level of the staircase-wise input. In each rat, the noise level of SNA measured after the administration of hexamethonium bromide was defined as zero. Because the absolute amplitude of SNA varied among animals depending on the recording conditions, mean SNA measured at the CSP level of 60 mm Hg in the first cycle was defined as 100 au (arbitrary units).

Static characteristics of the carotid sinus total-loop baroreflex (CSP–AP relationship), HR control (CSP–HR relationship), and neural arc (CSP–SNA relationship) approximated an inverse sigmoid curve, and were quantified using a four-parameter logistic function as follows (Kent et al., 1972):

$$y = \frac{P_1}{1 + \exp[P_2(\mathrm{CSP} - P_3)]} + P_4$$

where y denotes the output value (AP, HR, or SNA); P_1 is the response range of y; P_2 is the slope coefficient; P_3 is the midpoint of the sigmoid curve on the CSP axis; and P_4 is the minimum value of y. Although the slope of an inverse sigmoid curve is negative, for convenience sake, the maximum gain or slope of the logistic function (G_{max}) was calculated as a positive value of $P_1P_2/4$.

Static characteristics of the peripheral arc (SNA–AP relationship) approximated a straight line, and were quantified using a linear regression as follows:

$$\mathrm{AP} = a \times \mathrm{SNA} + b$$

where a and b represent the slope and intercept, respectively.

Statistical analysis

All data are presented as mean and SE values. Changes in each parameter obtained from 7 staircase-wise input cycles of 8 animals (56 values) were analyzed together by a multiple linear regression as follows (Glantz and Slinker, 2001):

$$p = C + B_{\mathrm{Time}} \times N + B_{\mathrm{VNS}} \times D_{\mathrm{VNS}} + B_1 \times D_1 + B_2 \times D_2 + \cdots + B_{k-1} \times D_{k-1}$$

where p is the parameter value; C is a constant term of the multiple linear regression; B_{Time} is a coefficient for the time effect; N is a cycle number ranging 0 (the first cycle) through 6 (the last cycle); B_{VNS} is a coefficient for the VNS effect; D_{VNS} is a dummy variable encoding VNS ($D_{\mathrm{VNS}} = 0$: no stimulation, $D_{\mathrm{VNS}} = 1$: during stimulation); D_1 through D_{k-1} are dummy variables encoding k different animals (see Table 1); and B_1 through B_{k-1} are coefficients for inter-individual variations. In the present study, because the time effect and VNS effect are of major concern, B_{Time} and B_{VNS} alone are reported together with C. Note that C predicts the parameter value in the first cycle ($N = 0$ and $D_{\mathrm{VNS}} = 0$) and serves as a reference value to interpret the magnitudes of the time effect and VNS effect. B_{Time} and B_{VNS} were tested whether they were significantly different from zero, with a significance level set at $P<0.05$ (Glantz and Slinker, 2001).

Table 1
Dummy variables encoding eight different animals.

	D_1	D_2	D_3	D_4	D_5	D_6	D_7
Animal 1	1	0	0	0	0	0	0
Animal 2	0	1	0	0	0	0	0
Animal 3	0	0	1	0	0	0	0
Animal 4	0	0	0	1	0	0	0
Animal 5	0	0	0	0	1	0	0
Animal 6	0	0	0	0	0	1	0
Animal 7	0	0	0	0	0	0	1
Animal 8	−1	−1	−1	−1	−1	−1	−1

To encode 8 different animals, only 7 different dummy variables are needed. An effect coding was used to model the inter-individual differences in a multiple linear regression analysis (Glantz and Slinker, 2001).

Results

Before starting the staircase-wise input protocol, CSP was matched to instantaneous AP through a servo control. Mean AP and HR under the carotid sinus baroreflex closed-loop conditions were 114.6 ± 5.3 mm Hg and 435.9 ± 11.7 beats/min, respectively. After the staircase-wise input protocol, hexamethonium bromide was administered, which decreased mean AP and HR to 54.0 ± 4.4 mm Hg and 350.9 ± 12.7 beats/min, respectively.

The left panels of Fig. 1 shows typical recordings of CSP, AP, HR, and SNA before, during, and after VNS in one animal. A white line in the SNA recording represents a 2-s moving averaged signal. The staircase-wise elevation in CSP decreased AP, HR, and SNA. VNS, applied at the 21st minute, immediately decreased HR, and thereafter HR remained decreased until the end of VNS at the 51st minute. The cessation of VNS returned HR toward the pre-stimulation level. VNS did not appear to affect the AP or SNA response. In the right panels of Fig. 1, the administration of hexamethonium bromide diminished SNA, which was followed by decreases in AP and HR.

The open-loop static characteristics of the carotid sinus total-loop baroreflex showed an inverse sigmoidal relationship regardless of VNS (Fig. 2, the top row). A multiple linear regression analysis on parameters of the total-loop baroreflex indicated that P_3 slightly decreased with time (0.8 mm Hg per cycle) (Table 2). Other parameters did not show a significant time effect. None of the parameters of the total-loop baroreflex showed a significant VNS effect.

The HR control also revealed an inverse sigmoidal relationship between CSP and HR regardless of VNS (Fig. 2, the second row). Although P_1 slightly decreased with time (1.7 beats/min per cycle), other parameters did not show a significant time effect (Table 2). VNS significantly decreased P_4 by 58.2 beats/min, and also decreased P_3 by 4.2 mm Hg. There was no significant VNS effect on P_1, P_2, or G_{max}.

The neural arc of the carotid sinus baroreflex showed an inverse sigmoidal relationship regardless of VNS (Fig. 2, the third row). The parameters of the neural arc except P_1 and G_{max} showed a significant time effect to some degree (Table 2). None of the parameters of the neural arc revealed a significant VNS effect.

The peripheral arc of the carotid sinus baroreflex approximated a straight line regardless of VNS (Fig. 2, the fourth row). There was no significant time effect on the slope or intercept of the peripheral arc (Table 2). VNS did not affect the slope, but significantly decreased the intercept by 5.8 mm Hg.

When the neural arc and the peripheral arc are drawn on a pressure–SNA plane, the intersection provides an operating point of the carotid sinus baroreflex (Fig. 2, the bottom row). While the operating-point AP did not change with time, the operating-point SNA increased slightly with time (1.3 au per cycle) (Table 2). VNS reduced the operating-point AP by 2.8 mm Hg without a significant effect on the operating-point SNA.

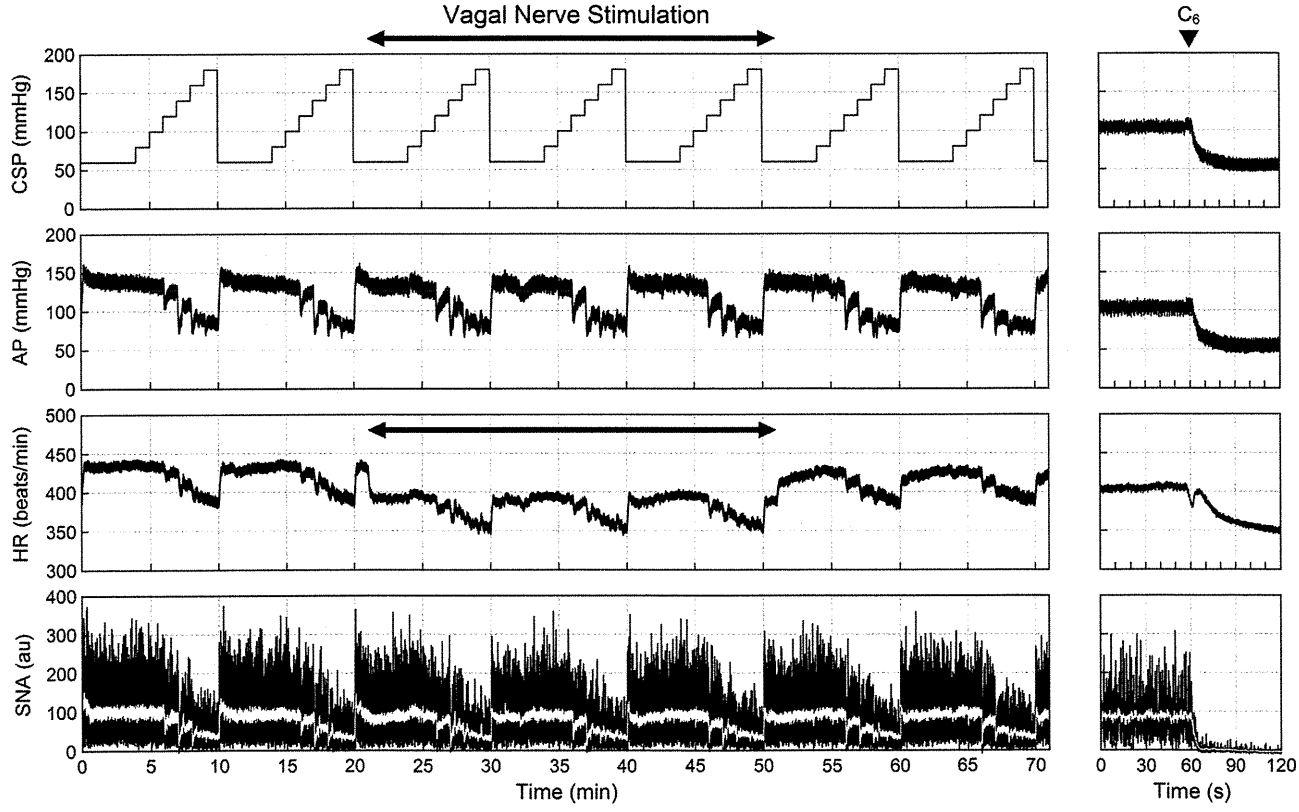

Fig. 1. Typical experimental recordings of carotid sinus pressure (CSP), arterial pressure (AP), heart rate (HR), and sympathetic nerve activity (SNA). A staircase-wise CSP input was repeated before, during, and after vagal nerve stimulation. The white line in the SNA recoding indicates a 2-s moving-averaged signal. The horizontal arrows indicate the duration of the vagal nerve stimulation. The right panels show the recordings of the intravenous bolus injection of hexamethonium bromide (C_6).

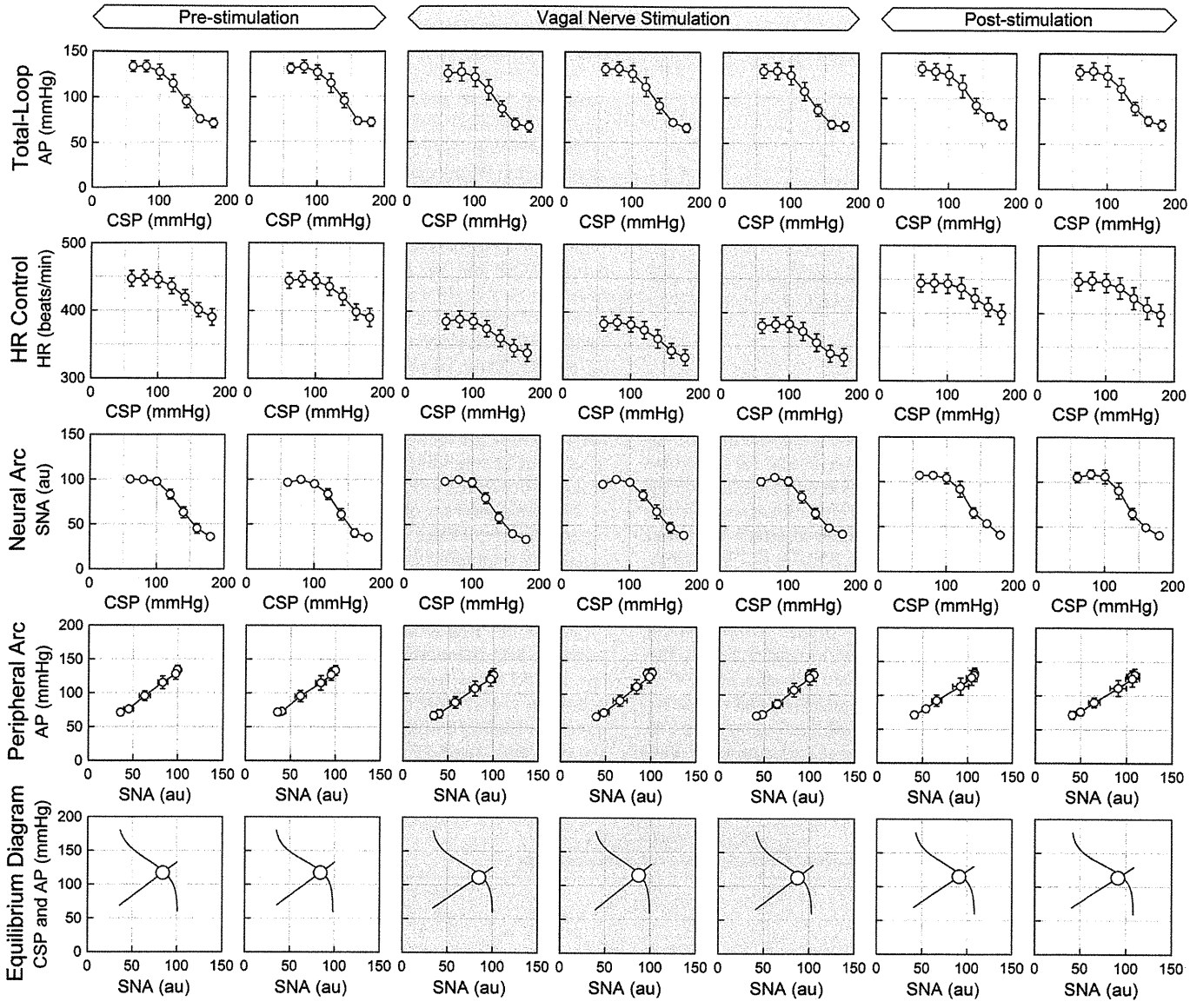

Fig. 2. The open-loop static characteristics of the carotid sinus total-loop baroreflex (top row), heart rate (HR) control (second row), neural arc (third row), peripheral arc (fourth row), and the baroreflex equilibrium diagram (bottom row). CSP: carotid sinus pressure, AP: arterial pressure, SNA: sympathetic nerve activity. The characteristics of the carotid sinus total-loop baroreflex, HR control, and neural arc approximated an inverse sigmoid curve. The characteristics of the peripheral arc approximated a straight line. The baroreflex equilibrium diagram was obtained by plotting the neural arc and peripheral arc on a pressure–SNA plane. The intersection of the two arcs (an open circle) indicates the operating point of the carotid sinus baroreflex.

Discussion

Interactions between the vagal and sympathetic systems

The efferent vagal nerve controls the heart via direct and indirect mechanisms (Kitamura et al., 2000; Mizuno et al., 2007). In the indirect mechanism, the vagal nerve antagonizes the sympathetic nerve at pre- and post-synaptic sites (Muscholl, 1980; Irisawa et al., 1993), producing significant vago-sympathetic interactions in controlling HR (Levy, 1971; Kawada et al., 1996). Although VNS reduces left ventricular contractility mainly via its negative chronotropic effect (Matsuura et al., 1997), it can also reduce the contractility via the antagonism to background sympathetic tone (Nakayama et al., 2001). These lines of evidence suggest that VNS would attenuate the sympathetic AP regulation depending on the level of SNA.

Contrary to our presumption, VNS, at an intensity of reducing HR by approximately 58 beats/min (13% of a closed-loop baseline HR), did not affect the carotid sinus total-loop baroreflex characteristics. The slope of the peripheral arc was not changed significantly during VNS, suggesting a preserved sympathetic AP regulation. On the other hand, the intercept of the peripheral arc was decreased significantly during VNS. The intercept, however, is estimated by a linear extrapolation of the SNA–AP relationship toward zero SNA. Because actually measured AP after ganglionic blockade was approximately 54 mm Hg and higher than the intercept, there should exist nonlinearity in the SNA–AP relationship as SNA approaches zero.

To assess the VNS effect within a linear range of the peripheral arc, the neural arc and peripheral arc were drawn on a single pressure–SNA plane (Fig. 2, the bottom row). The operating-point AP was decreased by 2.8 mm Hg during VNS, which was less than 3% of the reference value of 117 mm Hg (Table 2). Therefore, despite possible vago-sympathetic interactions in controlling HR (Levy, 1971; Kawada et al., 1996) and ventricular contractility (Nakayama et al., 2001), VNS may not acutely interfere with the carotid sinus baroreflex-mediated sympathetic AP regulation.

Table 2
Effects of time and vagal nerve stimulation (VNS) on parameters of the total baroreflex, heart rate (HR) control, neural arc, and peripheral arc.

	Constant (C)	Time effect (B_{Time})	VNS effect (B_{VNS})	R^2
Total baroreflex				
P_1, mm Hg	66.4 ± 2.5	−0.6 ± 0.5	0.2 ± 2.1	0.87
P_2, mm Hg^{-1}	0.085 ± 0.006	0.002 ± 0.001	0.001 ± 0.005	0.37
P_3, mm Hg	132.3 ± 1.4	−0.8 ± 0.3**	−1.5 ± 1.2	0.93
P_4, mm Hg	68.0 ± 2.1	0.3 ± 0.4	−3.0 ± 1.7	0.85
G_{max}, mm Hg/mm Hg	1.46 ± 0.07	0.01 ± 0.02	0.01 ± 0.06	0.89
HR control				
P_1, beats/min	61.6 ± 3.1	−1.7 ± 0.6*	−3.9 ± 2.6	0.76
P_2, mm Hg^{-1}	0.082 ± 0.006	0.001 ± 0.001	0.010 ± 0.006	0.54
P_3, mm Hg	138.2 ± 1.6	−0.3 ± 0.3	−4.2 ± 1.4**	0.90
P_4, beats/min	387.0 ± 5.8	1.6 ± 1.2	−58.2 ± 4.9**	0.87
G_{max}, beats min^{-1} mm Hg^{-1}	1.31 ± 0.08	−0.02 ± 0.02	0.02 ± 0.07	0.87
Neural arc				
P_1, au	68.6 ± 2.5	−0.5 ± 0.5	−2.6 ± 2.1	0.64
P_2, mm Hg^{-1}	0.082 ± 0.007	0.004 ± 0.001*	0.000 ± 0.006	0.46
P_3, mm Hg	135.9 ± 1.5	−1.0 ± 0.3**	−0.6 ± 1.2	0.92
P_4, au	29.6 ± 2.3	2.1 ± 0.5**	−0.6 ± 1.9	0.61
G_{max}, au/mm Hg	1.45 ± 0.13	0.05 ± 0.03	−0.09 ± 0.11	0.65
Peripheral arc				
Slope, mm Hg/au	0.98 ± 0.04	−0.01 ± 0.01	0.05 ± 0.03	0.59
Intercept, mm Hg	36.2 ± 2.4	−0.5 ± 0.5	−5.8 ± 2.0**	0.87
Operating point				
AP, mm Hg	117.7 ± 1.2	−0.5 ± 0.2	−2.8 ± 1.0**	0.94
SNA, au	82.5 ± 1.7	1.3 ± 0.4**	−1.1 ± 1.4	0.76

*$P<0.05$ and **$P<0.01$ by a multiple linear regression analysis. AP: arterial pressure, SNA: sympathetic nerve activity, au: arbitrary units.

VNS as a therapeutic approach

VNS has been shown to prevent lethal arrhythmia after acute myocardial ischemia in dogs (Vanoli et al., 1991). VNS, at an intensity of reducing HR by approximately 10%, can improve a long-term survival of chronic heart failure in rats (Li et al., 2004). Early short-term VNS also attenuates left ventricular remodeling in rabbits (Uemura et al., 2010). The antagonism to sympathetic overactivity through afferent (Kashihara et al., 2004) and efferent (Kawada et al., 2006, 2008) vagal pathways probably contribute to the treatment effects. β-Adrenergic blockade alone, however, cannot prevent the left ventricular remodeling in rats (Litwin et al., 1999), suggesting the importance of other mechanisms than β-adrenergic blockade. For instance, an anti-inflammatory effect through nicotinic receptors (Tracey, 2002; Altavilla et al., 2006) and an expression of tissue inhibitor of matrix metalloproteinase-1 through muscarinic receptors (Uemura et al., 2007) are reported.

Aside from the studies on treatment mechanisms, possible adverse effects of VNS need to be examined. Previous studies have demonstrated that the carotid sinus baroreflex function is depressed in canine heart failure (White, 1981; Wang et al., 1991). In chronic heart failure rats, the open-loop carotid sinus baroreflex function is depressed in such a way that AP becomes more labile to small pressure disturbances compared to normal rats (Kawada et al., 2010). If VNS further attenuated the sympathetic AP regulation, a serious adverse effect on the AP regulation could have followed. In the present study, whether efferent VNS affects sympathetic AP regulation was examined. The carotid sinus baroreflex-mediated sympathetic AP regulation was maintained during efferent VNS despite a significant bradycardic effect. In the case of VNS on the intact vagal nerve, activation of afferent vagal pathways may inhibit SNA. Whether afferent VNS modifies the carotid sinus baroreflex function was not examined in the present study and awaits further investigations.

Limitations

First, the effect of VNS on the carotid sinus baroreflex was examined in normal anesthetized and vagotomized rats. Because anesthesia affects the autonomic nerve activities, the results may not be directly extrapolated to the baroreflex function under conscious conditions. Second, VNS was applied continuously for 30 min and its acute effect was examined. Further studies are required to evaluate the effect of chronic VNS on the baroreflex function. Third, mechanisms for the contrasting effects of VNS on HR and AP were not clarified. It is likely that VNS, at an intensity used in the present study, did not affect venous return significantly, and a decrease in HR might have been counterbalanced by an increase in stroke volume to keep cardiac output similar regardless of VNS. Further studies are needed to verify this assumption. Fourth, increasing the intensity of VNS can reduce HR by more than 150 beats/min in rats (Mizuno et al., 2011), which may accompany significant hypotension such as that observed in rabbits (Shimizu et al., 2009). The effect of such a strong VNS on the baroreflex function is of physiological interest but beyond the scope of this study. Finally, considering the treatment use of VNS, it would be better to superimpose VNS over a native vagal tone. In the present study, however, we aimed to identify the possible effect of efferent VNS without an influence of afferent VNS using vagotomized rats. Although efferent VNS may simply replace the lost vagal tone, because vagal tone is thought to be diminished in heart failure, the present study may partly mimic the diseased conditions.

Conclusion

Although efferent VNS, at an intensity of treatment use, slightly decreased the intercept of the peripheral arc and the operating-point AP, it did not affect parameters of the carotid sinus total-loop baroreflex and the neural arc significantly, suggesting a limited ability of VNS to attenuate the sympathetic AP regulation. The present study would provide a rationale for the safety of VNS with regard to the carotid sinus baroreflex-mediated sympathetic AP regulation.

Conflict of interest statement

The authors declare that there are no conflicts of interest.

Acknowledgments

This study was supported by Health and Labour Sciences Research Grants (H19-nano-Ippan-009, H20-katsudo-Shitei-007, and H21-nano-Ippan-005) from the Ministry of Health, Labour and Welfare of Japan; the Grants-in-Aid for Scientific Research (C-23592319) promoted by the Ministry of Education, Culture, Sports, Science and Technology of Japan; and by the Industrial Technology Research Grant Program from the New Energy and Industrial Technology Development Organization (NEDO) of Japan.

References

Altavilla D, Guarini S, Bitto A, Mioni C, Giuliani D, Bigiani A, et al. Activation of the cholinergic anti-inflammatory pathway reduces NF-κB activation, blunts TNF-α production, and protects againts splanchic artery occlusion shock. Shock 2006;25: 500–6.

De Ferrari GM, Crijns HJ, Borggrefe M, Milasinovic G, Smid J, Zabel M, et al. for the CardioFit Multicenter Trial Investigators. Chronic vagus nerve stimulation: a new and promising therapeutic approach for chronic heart failure. Eur Heart J 2011;32: 847–55.

Glantz SA, Slinker BK. Primer of applied regression & analysis of variance. 2nd ed. New York: McGraw-Hill; 2001.

Ikeda Y, Kawada T, Sugimachi M, Kawaguchi O, Shishido T, Sato T, et al. Neural arc of baroreflex optimizes dynamic pressure regulation in achieving both stability and quickness. Am J Physiol 1996;271:H882–90.

Irisawa H, Brown HF, Giles W. Cardiac pacemaking in the sinoatrial node. Physiol Rev 1993;73:197–227.

Kamiya A, Kawada T, Shimizu S, Sugimachi M. Closed-loop spontaneous baroreflex transfer function is inappropriate for system identification of neural arc but partly accurate for peripheral arc: predictability analysis. J Physiol 2011;589: 1769–90.

Kashihara K, Kawada T, Li M, Sugimachi M, Sunagawa K. Bezold–Jarisch reflex blunts arterial baroreflex via the shift of neural arc toward lower sympathetic nerve activity. Jpn J Physiol 2004;54:395–404.

Kawada T, Ikeda Y, Sugimachi M, Shishido T, Kawaguchi O, Yamazaki T, et al. Bidirectional augmentation of heart rate regulation by autonomic nervous system in rabbits. Am J Physiol 1996;271:H288–95.

Kawada T, Sugimachi M, Sato T, Miyano H, Shishido T, Miyashita H, et al. Closed-loop identification of carotid sinus baroreflex open-loop transfer characteristics in rabbits. Am J Physiol 1997;273:H1024–31.

Kawada T, Yamazaki T, Akiyama T, Li M, Ariumi H, Mori H, et al. Vagal stimulation suppresses ischemia-induced myocardial interstitial norepinephrine release. Life Sci 2006;78:882–7.

Kawada T, Yamazaki T, Akiyama T, Kitagawa H, Shimizu S, Mizuno M, et al. Vagal stimulation suppresses ischemia-induced myocardial interstitial myoglobin release. Life Sci 2008;83:490–5.

Kawada T, Kamiya A, Li M, Shimizu S, Uemura K, Yamamoto H, et al. High levels of circulating angiotensin II shift the open-loop baroreflex control of splanchnic sympathetic nerve activity, heart rate and arterial pressure in anesthetized rats. J Physiol Sci 2009;59:447–55.

Kawada T, Li M, Kamiya A, Shimizu S, Uemura K, Yamamoto H, et al. Open-loop dynamic and static characteristics of the carotid sinus baroreflex in rats with chronic heart failure after myocardial infarction. J Physiol Sci 2010;60:283–98.

Kent BB, Drane JW, Blumenstein B, Manning JW. A mathematical model to assess changes in the baroreceptor reflex. Cardiology 1972;57:295–310.

Kitamura H, Yokoyama M, Akita H, Matsushita K, Kurachi Y, Yamada M. Tertiapin potently and selectively blocks muscarinic K^+ channels in rabbit cardiac myocytes. J Pharmacol Exp Ther 2000;293:196–205.

Levy MN. Sympathetic–parasympathetic interactions in the heart. Circ Res 1971;29: 437–45.

Li M, Zheng C, Sato T, Kawada T, Sugimachi M, Sunagawa K. Vagal nerve stimulation markedly improves long-term survival after chronic heart failure in rats. Circulation 2004;109:120–4.

Litwin SE, Katz SE, Morgan JP, Douglas PS. Effects of propranolol treatment on left ventricular function and intracellular calcium regulation in rats with postinfarction heart failure. Br J Pharmacol 1999;127:1671–9.

Matsuura W, Sugimachi M, Kawada T, Sato T, Shishido T, Miyano H, et al. Vagal stimulation decreases left ventricular contractility mainly through negative chronotropic effect. Am J Physiol 1997;273:H534–9.

Mizuno M, Kamiya A, Kawada T, Miyamoto T, Shimizu S, Sugimachi M. Muscarinic potassium channels augment dynamic and static heart rate responses to vagal stimulation. Am J Physiol Heart Circ Physiol 2007;293:H1564–70.

Mizuno M, Kawada T, Kamiya A, Miyamoto T, Shimizu S, Shishido T, et al. Exercise training augments the dynamic heart rate response to vagal but not sympathetic stimulation in rats. Am J Physiol Regul Integr Comp Physiol 2011;300:R969–77.

Mohrman DE, Heller LJ. Cardiovascular physiology. 6th ed. New York: McGraw Hill; 2006.

Muscholl E. Peripheral muscarinic control of norepinephrine release in the cardiovascular system. Am J Physiol 1980;239:H713–20.

Nakayama Y, Miyano H, Shishido T, Inagaki M, Kawada T, Sugimachi M, et al. Heart rate-independent vagal effect on end-systolic elastance of the canine left ventricle under various levels of sympathetic tone. Circulation 2001;104:2277–9.

Sato T, Kawada T, Inagaki M, Shishido T, Takaki H, Sugimachi M, et al. New analytic framework for understanding sympathetic baroreflex control of arterial pressure. Am J Physiol 1999a;276:H2251–61.

Sato T, Kawada T, Miyano H, Shishido T, Inagaki M, Yoshimura R, et al. New simple methods for isolating baroreceptor regions of carotid sinus and aortic depressor nerves in rats. Am J Physiol Heart Circ Physiol 1999b;276:H326–32.

Schwartz PJ. Vagal stimulation for heart diseases: from animals to men. — An example of translational cardiology. Circ J 2010;75:20–7.

Shimizu S, Akiyama T, Kawada T, Shishido T, Yamazaki T, Kamiya A, et al. In vivo direct monitoring of vagal acetylcholine release to the sinoatrial node. Auton Neurosci 2009;148:44–9.

Shoukas AA, Callahan CA, Lash JM, Haase EB. New technique to completely isolate carotid sinus baroreceptor regions in rats. Am J Physiol Heart Circ Physiol 1991;260:H300–3.

Tracey KJ. The inflammatory reflex. Nature 2002;420:853–9.

Uemura K, Li M, Tsutsumi T, Yamazaki T, Kawada T, Kamiya A, et al. Efferent vagal nerve stimulation induces tissue inhibitor of metalloproteinase-1 in myocardial ischemia–reperfusion injury in rabbit. Am J Physiol Heart Circ Physiol 2007;293: H2254–61.

Uemura K, Zheng C, Li M, Kawada T, Sugimachi M. Early short-term vagal nerve stimulation attenuates cardiac remodeling after reperfused myocardial infarction. J Card Fail 2010;16:689–99.

Vanoli E, De Ferrari GM, Stramba-Badiale M, Hull Jr SS, Foreman RD, Schwartz PJ. Vagal stimulation and prevention of sudden death in conscious dogs with a healed myocardial infarction. Circ Res 1991;68:1471–81.

Wang W, Chen JS, Zucker IH. Carotid sinus baroreceptor reflex in dogs with experimental heart failure. Circ Res 1991;68:1294–301.

White CW. Abnormalities in baroreflex control of heart rate in canine heart failure. Am J Physiol 1981;240:H793–9.

J Physiol Sci (2011) 61:457–465
DOI 10.1007/s12576-011-0166-7

ORIGINAL PAPER

Norwood procedure with non-valved right ventricle to pulmonary artery shunt improves ventricular energetics despite the presence of diastolic regurgitation: a theoretical analysis

Shuji Shimizu · Dai Une · Toshiaki Shishido · Atsunori Kamiya · Toru Kawada · Shunji Sano · Masaru Sugimachi

Received: 17 May 2011 / Accepted: 10 July 2011 / Published online: 10 August 2011

Abstract When the Norwood procedure is conducted for the hypoplastic left heart syndrome using a non-valved right ventricle (RV) to pulmonary artery (PA) shunt, diastolic regurgitation from PA to RV may have an adverse effect on postoperative hemodynamics. In this study, we examined the impact of the diastolic regurgitation on ventricular energetics by computational analysis using a combination of a time-varying elastance chamber model and a modified three-element Windkessel vascular model. This study revealed that use of the valved or non-valved RV-PA shunt eliminated pulmonary over-circulation which was observed when using the systemic to pulmonary artery shunt (modified Blalock–Taussig shunt). Although the valved RV-PA shunt improved pulmonary blood supply and consequently increased pulmonary artery flow and oxygen saturation compared to the non-valved RV-PA shunt, the non-valved RV-PA shunt improved ventricular energetics in spite of the presence of PA to RV regurgitation.

Keywords Hypoplastic left heart syndrome · Norwood procedure · Right ventricle to pulmonary artery shunt · Ventricular energetics · Valved · Computational model

S. Shimizu (✉) · D. Une · T. Shishido · A. Kamiya · T. Kawada · M. Sugimachi
Department of Cardiovascular Dynamics, National Cerebral and Cardiovascular Center Research Institute, 5-7-1 Fujishiro-dai, Suita, Osaka 565-8565, Japan
e-mail: shujismz@ri.ncvc.go.jp

S. Shimizu · S. Sano
Department of Cardiovascular Surgery, Okayama University Graduate School of Medicine, Dentistry and Pharmaceutical Sciences, Okayama, Japan

Introduction

The outcome of the Norwood procedure for hypoplastic left heart syndrome (HLHS) has improved in the past several decades. Previously, pulmonary circulation was maintained by a systemic to pulmonary artery shunt (SPS), such as the modified Blalock–Taussig shunt. However, the SPS has the drawback of systemic-to-pulmonary diastolic run-off, which causes a massive increase in ventricular preload. The development of the right ventricle to pulmonary artery (RV-PA) shunt may have contributed to the dramatic improvement in clinical outcome of recent years, because the RV-PA shunt eliminates the diastolic run-off and increases diastolic systemic arterial pressure (SAP). This increase in diastolic SAP may improve coronary blood supply [1]. Furthermore, the RV-PA shunt may reduce myocardial oxygen demand. Bove et al. [2] reported that the RV-PA shunt decreased stroke work and improved right ventricular energetics.

The RV-PA shunt may be classified into valved and non-valved. The non-valved RV-PA shunt is associated with diastolic regurgitation from PA to RV. This regurgitation may increase RV preload and myocardial oxygen demand compared to the valved RV-PA shunt. Therefore, preventing diastolic regurgitation using the valved conduit may further improve clinical outcome. Reihartz et al. [3] reported that use of a homograft valved RV-PA conduit was associated with low early mortality. Takeuchi et al. [4] used a valved saphenous vein homograft and also reported improved right ventricular function. However, whether the non-valved RV-PA shunt truly improves the outcome of the Norwood procedure compared to the SPS, and whether the valved RV-PA shunt further improves the outcome compared to the non-valved RV-PA shunt remain controversial.